Geologic Map of the Yacolt Quadrangle, Clark County, Washington

By Russell C. Evarts

Pamphlet to accompany
Scientific Investigations Map 2901

2006

U.S. Department of the Interior
U.S. Geological Survey

INTRODUCTION

GEOGRAPHIC AND GEOLOGIC SETTING

The Yacolt 7.5' quadrangle is situated in the foothills of the western Cascade Range of southwestern Washington approximately 35 km northeast of Portland, Oregon (fig. 1). Since late Eocene time, the Cascade Range has been the locus of an active volcanic arc associated with underthrusting of oceanic lithosphere beneath the North American continent along the Cascadia Subduction Zone. Volcanic and shallow-level intrusive rocks emplaced early in the history of the arc underlie most of the Yacolt quadrangle, forming a dissected and partly glaciated terrain with elevations between 250 and 2180 ft (75 and 665 m). The bedrock surface slopes irregularly but steeply to the southwest, forming the eastern margin of the Portland Basin, and weakly consolidated Miocene and younger basin-fill sediments lap up against the bedrock terrain in the southern part of the map area. A deep canyon, carved by the East Fork Lewis River that flows westward out of the Cascade Range, separates Yacolt and Bells Mountains, the two highest points in the quadrangle. Just west of the quadrangle, the river departs from its narrow bedrock channel and enters a wide alluvial floodplain. In the northeast part of the quadrangle, the town of Yacolt resides in a linear, glacial-outwash-filled basin of probable tectonic origin.

The Portland Basin is part of the Puget-Willamette Lowland that separates the Cascade Range from the Oregon Coast Range (fig. 1A). The Portland Basin has been interpreted as a pull-apart basin located in the releasing stepover between two en echelon, northwest-striking, right-lateral fault zones (Beeson and others, 1985, 1989; Yelin and Patton, 1991; Blakely and others, 1995). These fault zones are thought to reflect regional transpression and dextral shear within the forearc in response to oblique subduction of the Pacific Plate along the Cascadia Subduction Zone (Pezzopane and Weldon, 1993; Wells and others, 1998). The southwestern margin of the Portland Basin (fig. 1B) is a well-defined topographic break along the base of the Tualatin Mountains, which form an asymmetric anticlinal ridge bounded on its northeast flank by the Portland Hills Fault Zone (Balsillie and Benson, 1971; Beeson and others, 1989; Blakely and others, 1995). This fault zone is believed to be an active structure (Wong and others, 2001; Liberty and others, 2003). The nature of the corresponding northeastern margin of the basin is less clear, but a poorly defined and partially buried dextral extensional structure has been hypothesized from topography, microseismicity, potential field-anomalies, and reconnaissance geologic mapping (Yelin and Patton, 1991; Beeson and others, 1989; Blakely and others, 1995).

This map is a contribution to a program designed to improve the geologic database for the Portland Basin region of the Pacific Northwest urban corridor, the densely populated Cascadia forearc region of western Washington and Oregon. Better and more detailed information on the bedrock and surficial geology of the basin and its surrounding area is needed to refine assessments of seismic risk (Yelin and Patton, 1991; Bott and Wong, 1993), ground-failure hazards (Madin and Wang, 1999; Wegmann and Walsh, 2001) and resource availability in this rapidly growing region.

PREVIOUS GEOLOGIC INVESTIGATIONS

Previous geologic mapping in the Yacolt area, generally carried out as part of broad regional reconnaissance investigations, established the basic stratigraphic framework and distribution of geologic units in the quadrangle. The first systematic geologic work within the quadrangle was that of Mundorff (1964), who mapped the area for a water-resources evaluation of Clark County. His 1:48,000-scale geologic map accurately portrays contacts between Tertiary bedrock and the basin-fill units and his report gives detailed descriptions of the basin-fill deposits. Mundorff (1984) discussed the Pleistocene glacial deposits of the lower Lewis River valley in some detail, and named these deposits the Amboy Drift.

Swanson and others (1993) updated Mundorff's Clark County work as part of an investigation of ground-water resources throughout the Portland Basin. Their work focused on the basin-fill units, and their map shows hydrogeologic rather than stratigraphic units, although there is substantial equivalence between the two. They analyzed lithologic logs of 1500 water wells to produce a series of maps that show the elevations and thicknesses of hydrogeologic units throughout the basin, thus constructing a rough 3-dimensional view of the subsurface stratigraphy of the basin fill. Phillips (1987) compiled a 1:100,000-scale geologic map of the Vancouver 30'x60' quadrangle, which includes the Yacolt 7.5' quadrangle, as part of the state geologic map program of the Washington Division of Geology and Earth Resources (Walsh and others, 1987). Although relying heavily on Mundorff's work, he did undertake some original reconnaissance mapping and his was the first map to show major lithostratigraphic units within the Tertiary bedrock sequence. He acquired chemical analyses for some of the volcanic rocks of the region as well as a few whole-rock K-Ar age determinations, although none of these new data were obtained from the Yacolt quadrangle.

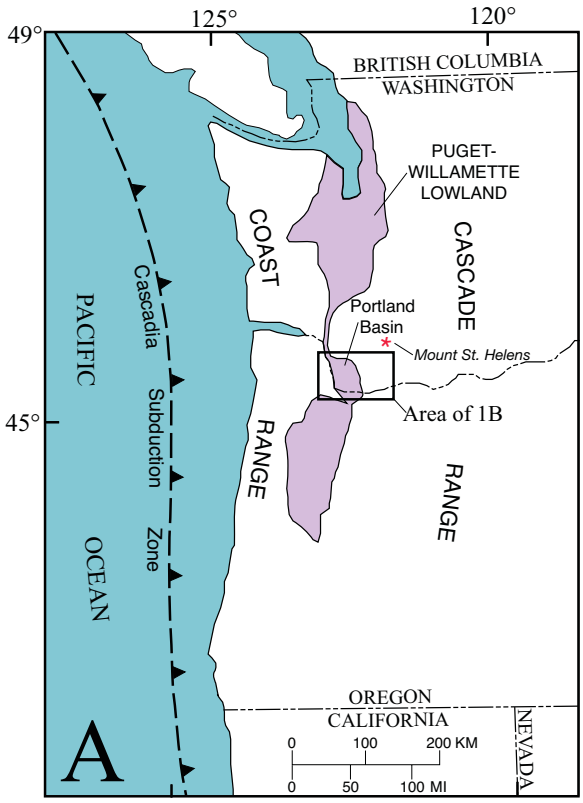

Figure 1A. Regional setting of the Yacolt quadrangle showing major tectonic and physiographic features of the Pacific Northwest.

ACKNOWLEDGMENTS

Access granted by landowners was essential for mapping in the Yacolt quadrangle. I thank Dennis Mohan of the Longview Fibre Company and Brian Poehlein of the Washington Division of Natural Resources for permission to work on their timberlands in the eastern half of the quadrangle. Diane M. Johnson of Washington State University performed chemical analyses and Robert Fleck of the U.S. Geological Survey determined $^{40}Ar/^{39}Ar$ ages. Andrei Sarna-Wojcicki, Kenneth Bishop, Judith Fierstein, and Michael Clynne made available essential laboratory facilities. Tammy Howes of the Washington Department of Ecology Southwest Regional Office in Lacey, Wash., provided access to files of water-well drillers' logs. Connie Manson helped obtain unpublished information from the library at the Washington Division of Geology and Earth Resources in Olympia, Wash. I have benefited immensely from discussions on various aspects of the regional stratigraphy, structure, and geologic history of southwestern Washington with Roger Ashley, Michael Clynne, Paul Hammond, Alan Niem, Jim O'Connor, William Phillips, William Scott, James Smith, Donald Swanson, Karl Wegmann, and Ray Wells. Geologic mapping of the Yacolt quadrangle was initiated in 1998 by Keith Howard, who freely shared field notes, thin sections, a preliminary map, and shared his insights and interpretations. I thank Russell Graymer and Andrei Sarna-Wojcicki for their prompt and thoughtful technical reviews.

SYNOPSIS OF GEOLOGY

Bedrock of the Yacolt quadrangle consists of near-horizontal strata of Oligocene volcanic and volcaniclastic rocks that comprise early products of the Cascade volcanic arc. Basalt and basaltic andesite flows predominate. Most were emplaced on the flanks of a large mafic shield volcano and are interfingered with crudely bedded sections of volcanic breccia of probable lahar origin and a variety of well bedded epiclastic sedimentary rocks. Bedrock is poorly exposed, particularly north of the East Fork Lewis River where it is extensively

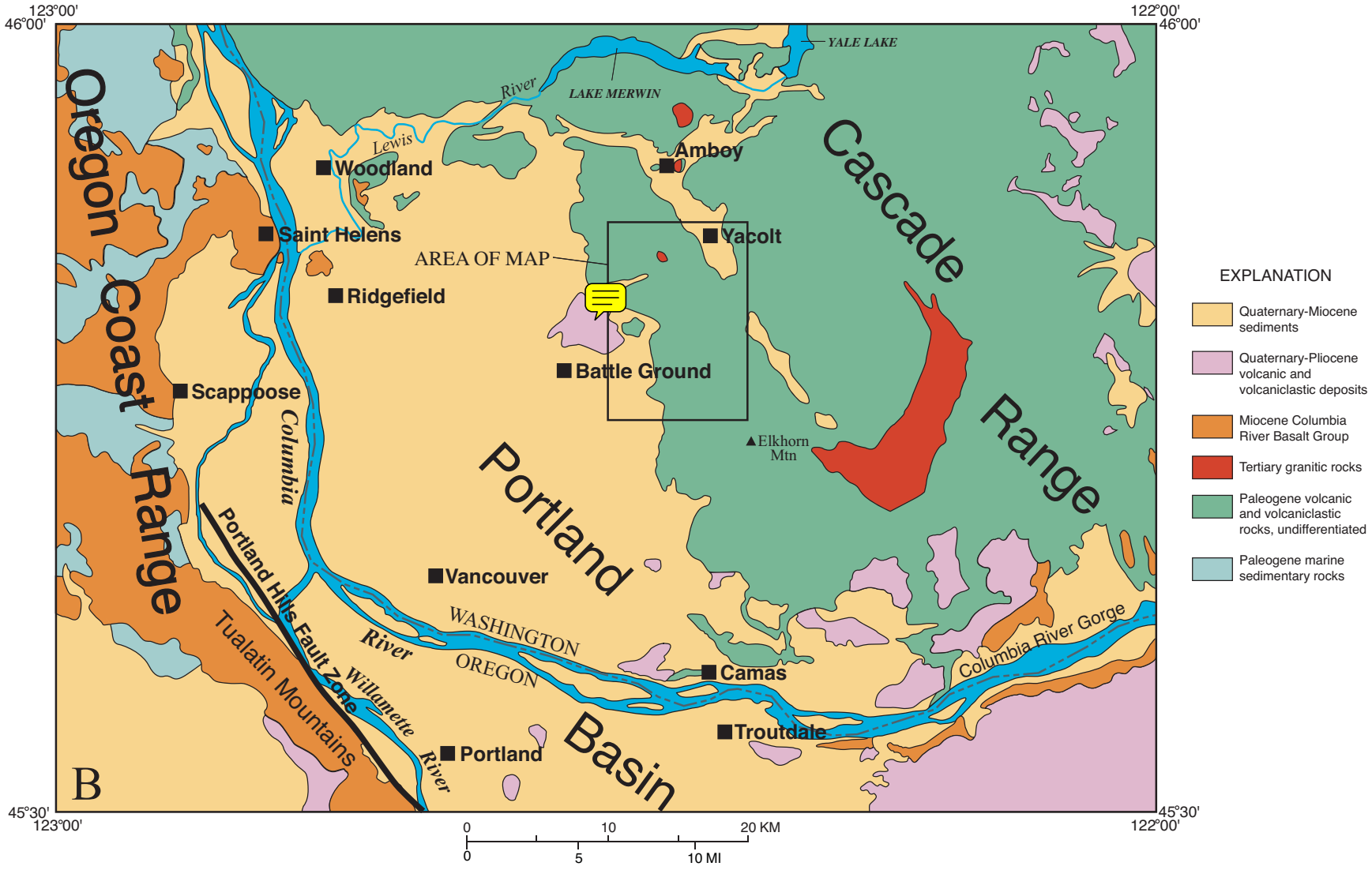

Figure 1B. Simplified geologic map of the Vancouver 30' x 60' quadrangle, modified from Phillips (1987a).

covered by Quaternary till. At Yacolt Mountain, the volcanogenic rocks are intruded by a body of Miocene quartz diorite that is compositionally distinct from any volcanic rocks in the map area. The town of Yacolt sits in a north-northwest-trending valley apparently formed within a major fault zone. Several times during the Pleistocene, mountain glaciers moved down the Lewis River valley (Crandell and Miller, 1974; Mundorff, 1984) and spread southward into the map area. The largest glacier(s) covered the entire map area north of the East Fork Lewis River except for the summit of Yacolt Mountain. As the ice receded, it left behind a sculpted bedrock topography thickly mantled by drift, and deposited outwash in the fault-bounded valley at Yacolt and along the East Fork Lewis River valley.

Because of the extensive drift cover, deep weathering, and dense vegetation of the region, natural outcrops in the map area are generally limited to steep cliff faces, landslide scarps, and streambeds; many exposures are in roadcuts and quarries. Surface information was supplemented with lithologic data obtained from several hundred water-well reports in the files of the Washington Department of Ecology; well locations were taken as described in the reports and were not field checked, but only wells considered reliably located were used to infer the distribution and thicknesses of units in the subsurface.

PALEOGENE BEDROCK

Lithostratigraphic nomenclature for the stratigraphically complex Tertiary volcanic rocks of the southern Washington Cascade Range is poorly developed. Formal names have been proposed for Paleogene volcanic strata in several widely scattered locations (Wilkinson and others, 1946; Snavely and others, 1958; Roberts, 1958; Trimble, 1963; Fiske and others, 1963). However, these formations have proven to be only locally important or to be so broadly defined as to be essentially synonymous with Tertiary volcanic rocks (Evarts and others, 1987; Smith, 1993). In order to show as much detail as possible without generating a proliferation of local lithostratigraphic units, this and previously published maps of the Portland Basin (Evarts, 2004a, b, c, 2005) portray primarily lithologic rather than lithostratigraphic units, although informal lithostratigraphic names are used where appropriate.

VOLCANIC AND VOLCANICLASTIC ROCKS

Mapping and geochronologic data from the Yacolt and adjacent quadrangles (Evarts, 2005; R.C. Evarts and R.J. Fleck, unpub. data) indicate that the Oligocene section here contains a significant unconformity, possibly of regional extent. The unconformable contact, a surface of modest relief located at the base of the basaltic andesite of Elkhorn Mountain, is mostly buried by till or other surficial deposits but is locally exposed along the East Fork Lewis River.

Strata below the unconformity

The stratigraphic section beneath the unconformity that crops out along the banks of the East Fork Lewis River consists of volcaniclastic rocks (Tvso) interbedded with basaltic andesite flows and zeolitic flow breccia (Tba) and capped by a thick red paleosol. These strata consist chiefly of texturally and compositionally immature siltstone, sandstone, grit, conglomerate, and breccia, largely of epiclastic origin. Most of the clasts in these rocks were derived from erosion of older extrusive rocks or reworked from unconsolidated penecontemporaneous airfall and ash-flow deposits. Fragments of volcanic rocks petrographically similar to interbedded lava flows are the dominant constituents of most beds; less abundant components include plagioclase, Fe-Ti oxides, and pyroxene crystals, pumice, vitric ash, and fine-grained dioritic rocks. Plant remains, including some well preserved fossil leaves, are widely dispersed in sandy and silty beds, and thin coal beds are locally present.

The volcaniclastic debris was probably deposited in rivers and lakes of low-lying terrain between volcanic edifices. Lahars and other debris flows that moved down the volcano flanks are recorded by interbeds of tuff breccia and lithic lapilli tuff, some of which contain charred wood and fossilized logs. The paucity of pumiceous or welded tuffs indicates that most eruptions were nonexplosive. Near the north boundary of the map area, andesite flows (Ta) form isolated outcrops within till-mantled terrain. They are interpreted as pre-Elkhorn Mountain rocks that formed a paleotopographic high, which was surrounded and eventually buried by the mafic lava flows.

A fossil flora collected from strata just downstream of the bridge north of Heisson was assigned a late Eocene age by R.W. Brown (Trimble, 1963). However, an $^{40}Ar/^{39}Ar$ age of 31.9±1.2 Ma (table 2) obtained from a porphyritic basaltic andesite flow interbedded with volcaniclastics upstream from Lucia Falls indicates that the fossil assemblage is more likely early Oligocene. This age is consistent with ages of about 33 Ma obtained from stratigraphically lower ignimbrites in the Amboy quadrangle to the north (Evarts, 2005).

Basaltic andesite of Elkhorn Mountain

Basalt and basaltic andesite flows and flow breccia that dominate the Paleogene section of the Yacolt quadrangle constitute a petrographically and

chemically coherent suite of tholeiitic lavas that is herein informally named the basaltic andesite of Elkhorn Mountain (Tbem) after a peak about 1 km south of the southeastern corner of the Yacolt quadrangle. This package of flows has a maximum thickness of at least 800 m and extends southward as far as Camas, about 20 km south of the quadrangle (R.C. Evarts, unpub. mapping). These flows were probably emplaced on the flank of a large shield volcano. No dikes have been found in the map area, so source vents must lie outside the map area, most likely to the east. Individual flows are typically 4 to 10 m thick but locally reach 70 m thick; single flows can be traced for distances of as much as 7 km. They are characterized by blocky, platy, or columnar-jointed interiors that commonly grade into upper and lower flow breccia zones. The upper zones typically contain abundant zeolite-, quartz-, and clay-filled vesicles and have been oxidized to reddish-orange colors during cooling. All flows were apparently emplaced subaerially; many rest on thin red paleosols developed on previously emplaced flows or on sedimentary intervals, and no pillow lavas or other indications of subaqueous environments were observed.

Flows in the Elkhorn Mountain unit range from aphyric to highly porphyritic. Aphyric and sparsely phyric flows commonly exhibit a closely spaced platy parting that is parallel to the alignment of feldspar microlites observed in thin section. Seriate to porphyritic flows contain phenocrysts of plagioclase and olivine, with or without augite, in an intergranular to trachytic groundmass. Extremely porphyritic to glomerophyric basalts are scattered throughout the basaltic andesite of Elkhorn Mountain, some so packed with coarse blocky plagioclase phenocrysts (as much as 55 percent) that they macroscopically resemble phaneritic intrusive rocks. Widely spaced rectilinear joints typify these flows, which tend to weather into spheroids 1 to 3 m across. The plagioclase phenocrysts in these rocks are larger than 5 mm and commonly larger than 1 cm across and are nearly unzoned; many are anhedral and appear to have been broken or partly resorbed. Groundmass textures indicate the basalts cooled rapidly; their coarse-grained appearance reflects pre-eruptive accumulation and concentration of feldspar crystals in a subvolcanic magma chamber rather than slow cooling at depth.

Lava flows of the basaltic andesite of Elkhorn Mountain vary in composition from basalt to mafic andesite, but most are basaltic andesite; they are uniformly tholeiitic, with low to medium potassium contents (fig. 2). The densely plagioclase-phyric basalts exhibit exceptionally high Al_2O_3 contents (as high as 22.5 wt percent), that correlate with the abundance of plagioclase phenocrysts (fig. 3a). All rocks with more than about 18 percent Al_2O_3, including most of the basalts (fig. 3b), probably accumulated plagioclase crystals prior to eruption. Compared to mafic flows elsewhere in the southern Washington Cascade Range (Evarts and Ashley, 1990a,b, 1991, 1992; Evarts and Bishop, 1994; Evarts and Swanson, 1994; Evarts, 2001, 2002, 2004a, b, 2005; R.C. Evarts, unpub. data), the Elkhorn Mountain flows are unusually rich in Fe (about 8.8 to 12.8 wt percent FeO* in flows without excess feldspar; fig. 3c) and poor in Sr (generally less than 320 ppm Sr in flows without excess feldspar; fig. 3d). Incompatible-element ratios such as Ba/Nb (about 20), Ba/Zr (about 1.5) and Zr/Nb (about 13.5) vary little throughout the suite (fig. 4), suggesting that all the lavas are related primarily by fractional crystallization processes.

A basalt flow from the stratigraphically highest part of the unit in the map area, at the summit of Bells Mountain, gave a whole-rock $^{40}Ar/^{39}Ar$ age of 27.1±0.1 Ma (table 2). Similar ages have been obtained from an associated dacite (see below) as well as from basaltic andesite flows in this unit to the south (R.J. Fleck, written commun., 2005).

Dacite

Glomerophyric pyroxene dacite (Td) forms a thick lobate flow interbedded with basaltic andesites and volcaniclastic rocks on the ridge that extends northwest from Bells Mountain. This dacite is chemically distinct from the basaltic andesite of Elkhorn Mountain (fig. 2) but possesses similar ratios of incompatible trace elements (fig. 4), suggesting that it is a differentiate of the same magma. Given the limited extent of the flow and the high viscosity of silicic magma, the dacite probably erupted from a nearby satellitic vent on the flank of the large mafic shield. Plagioclase from this unit yielded an $^{40}Ar/^{39}Ar$ age of 26.5±0.1 Ma (table 2), similar in age to the dated basaltic andesite flow.

Volcaniclastic rocks

Above the Oligocene unconformity, volcaniclastic rocks (Tvs and Tvb) are much less abundant than lava flows. The clastic rocks are more pervasively altered and weathered than the associated flows, and consequently are less commonly exposed. Well-bedded epiclastic strata (Tvs) interfinger with basal flows of the basaltic andesite of Elkhorn Mountain near the East Fork Lewis River but are uncommon elsewhere.

On the flanks of Bells Mountain, thick beds of massive volcanic breccia (Tvb) dominate a westward thickening section that ranges from about 70 m to more than 250 m thick. Intense weathering is characteristic of the fragmental deposits, and they are best exposed in headwall scarps of numerous

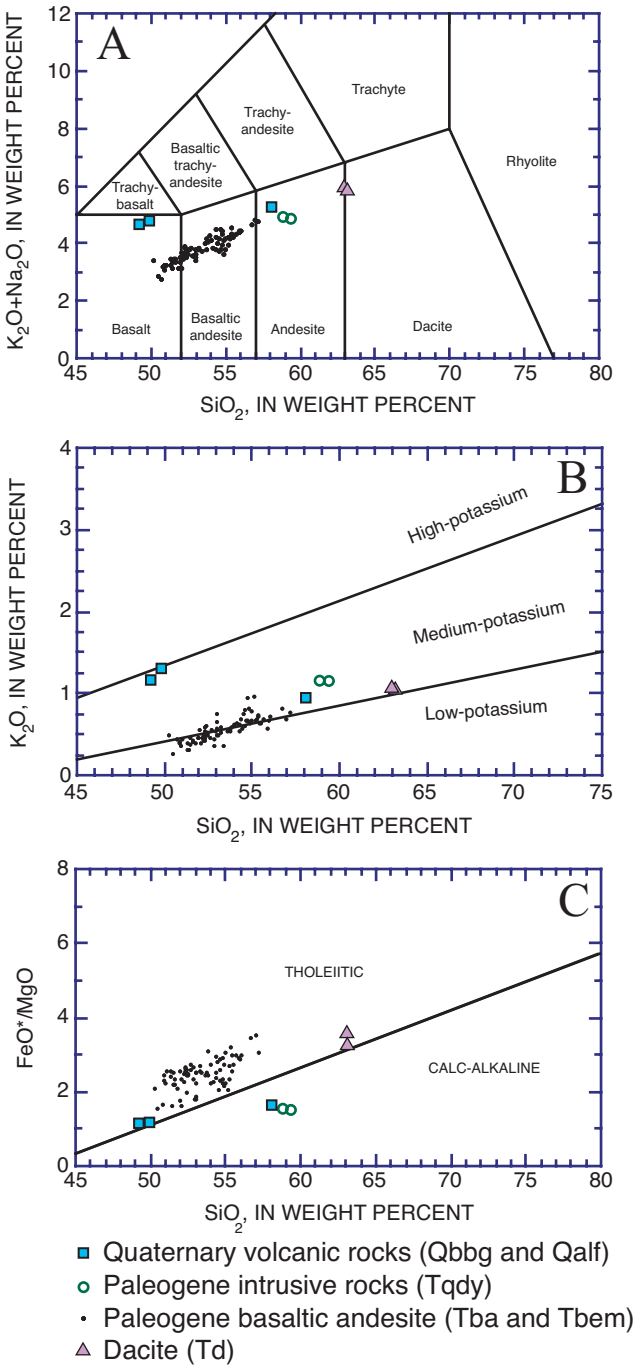

Figure 2. Chemical characteristics of volcanic rocks from the Yacolt 7.5' quadrangle (analyses recalculated volatile-free). A, K_2O+Na_2O versus SiO_2, showing IUGS classification (Le Maitre, 2002); B, K_2O versus SiO_2, showing low-, medium-, and high-potassium fields extrapolated from Gill (1981, p. 6); C, FeO*/MgO versus SiO_2, showing classification into tholeiitic and calc-alkaline rocks according to Miyashiro (1974). FeO*, total Fe as FeO.

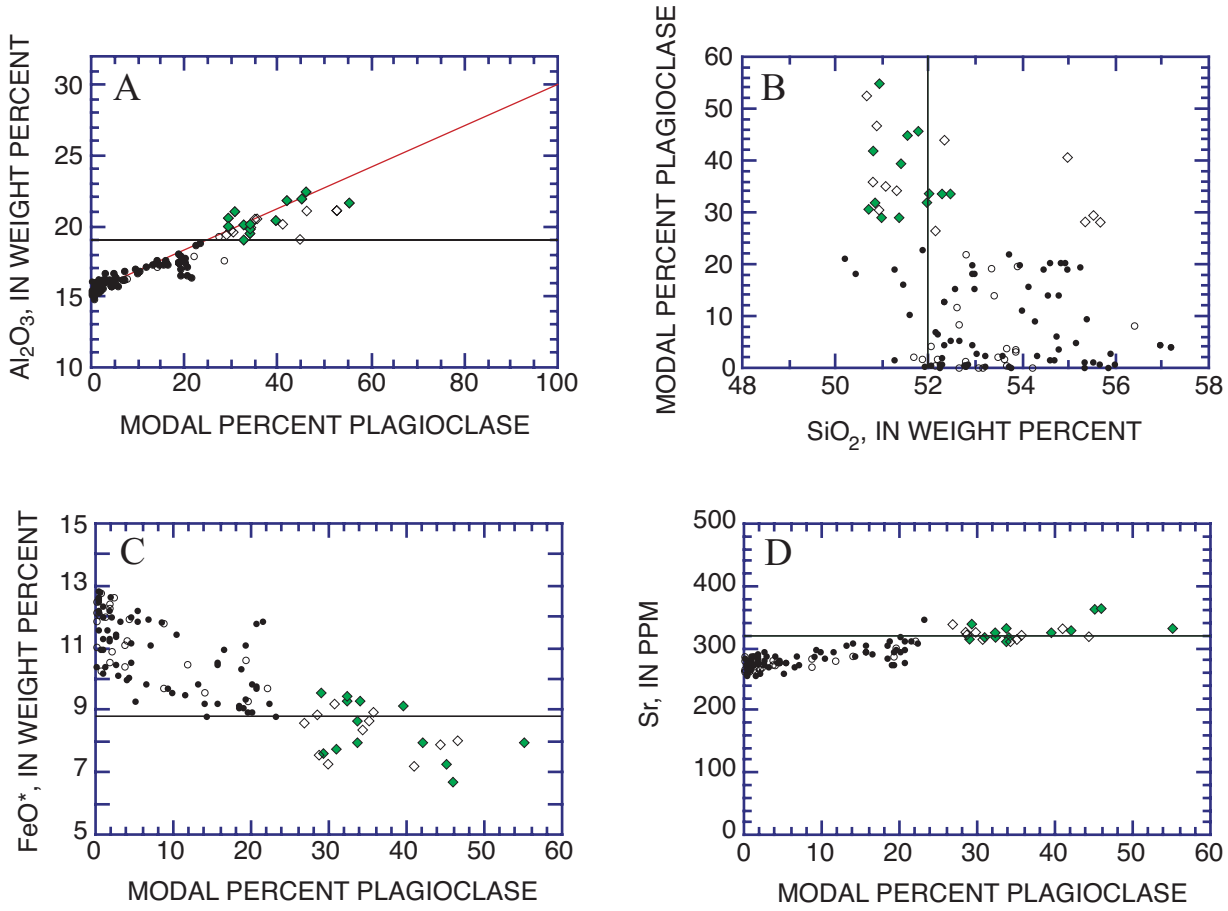

Figure 3. Chemical characteristics of lavas in the basaltic andesite of Elkhorn Mountain, illustrating the effects of plagioclase accumulation. Filled symbols designate samples from Yacolt quadrangle, unfilled symbols designate samples from adjacent areas; strongly plagioclase-accumulative samples, shown as diamonds, contain more than 25 percent plagioclase phenocrysts. *A*, Al_2O_3 versus abundance of plagioclase phenocrysts, showing that the lavas plot along a plagioclase-accumulation line (shown in red) that projects to the composition of a calcic labradorite (about 30 wt percent Al_2O_3); *B*, SiO_2 versus abundance of plagioclase phenocrysts, showing that many basalts (SiO_2 less than 52 percent) are strongly plagioclase-accumulative lavas; *C*, FeO* versus abundance of plagioclase phenocrysts, showing that FeO* contents of most non-accumulative lavas are greater than 8.8 percent; FeO*, total Fe as FeO; *D*, Sr versus abundance of plagioclase phenocrysts, showing that Sr contents of non-plagioclase accumulative lavas are mostly less than 320 ppm.

landslides generated by failure of clay-rich breccia. The typical bed in this unit is a polylithologic, matrix-supported, tuff breccia that contains subrounded to angular blocks generally less than 1 m but locally 10 m or more in diameter. Most of the clasts resemble associated mafic flows (table 1, nos. 15 and 63). Most of these beds were probably deposited by lahars or other types of debris flows, but an indurated monolithic tuff breccia that crops out on the southwest side of Bells Mountain may have been emplaced as a hot block-and-ash flow.

QUARTZ DIORITE OF YACOLT MOUNTAIN

The only intrusive rock mapped in the quadrangle is a stock of seriate to pyroxene quartz diorite (Tqdy) that underlies Yacolt Mountain. The quartz diorite is a seriate to hypidiomorphic granular rock that contains euhedral to subhedral crystals of plagioclase, augite, hypersthene, olivine, and Fe-Ti oxide in a matrix of fine-grained smectite, intergrowths of quartz and potassium feldspar and minor local hornblende, biotite and apatite. This unit includes a dark porphyritic rock with locally devitrified groundmass that crops out in the creek valley southeast of Yacolt Mountain. Despite the petrographic differences, the fine-grained and coarse-grained rocks are chemically indistinguishable (table 1, nos. 81 and 82; fig. 2) and the porphyritic rock is interpreted as a chilled border phase of the intrusion. The quartz diorite of Yacolt Mountain is chemically distinguished from all other Paleogene rocks in the

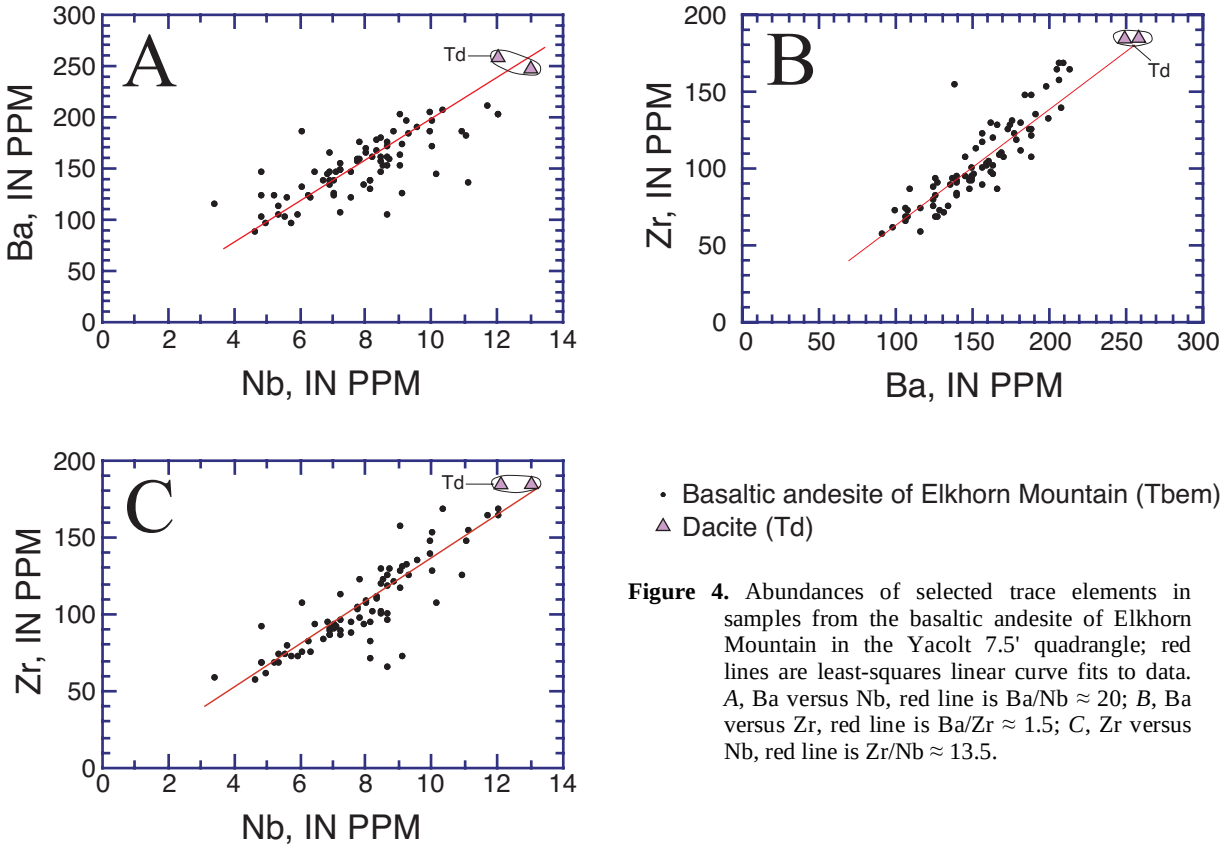

Figure 4. Abundances of selected trace elements in samples from the basaltic andesite of Elkhorn Mountain in the Yacolt 7.5' quadrangle; red lines are least-squares linear curve fits to data. *A*, Ba versus Nb, red line is Ba/Nb ≈ 20; *B*, Ba versus Zr, red line is Ba/Zr ≈ 1.5; *C*, Zr versus Nb, red line is Zr/Nb ≈ 13.5.

map area by its calcalkaline composition and higher contents of K, Sr, and Ba (fig. 2; table 1). Plagioclase separated from the border phase yielded an $^{40}Ar/^{39}Ar$ age of 21.5±0.1 Ma (table 2).

METAMORPHISM AND HYDROTHERMAL ALTERATION

The Oligocene rocks in the Yacolt quadrangle have been subjected to zeolite-facies regional metamorphism, the general character of which is similar to that described from other areas in the southern Washington Cascade Range (Fiske and others, 1963; Wise, 1970; Evarts and others, 1987; Evarts and Swanson, 1994). This region-wide metamorphism reflects burial of the Oligocene strata by younger volcanic rocks within the relatively high-heat-flow environment of an active volcanic arc.

In rocks subjected to zeolite-facies metamorphism, the extent of replacement of igneous minerals by secondary phases ranges from incipient to complete. Permeable volcaniclastic rocks are the most susceptible to zeolitization, whereas intercalated massive lava flows may be only slightly affected. In lava flows of mafic to intermediate composition, the primary effect of very-low-grade metamorphism is the nearly universal development of clay minerals and zeolites that replace labile interstitial glass, fill vesicles, and coat joint surfaces. Feldspar typically displays partial alteration along fractures and cleavage planes to clay minerals and (or) zeolites. Olivine phenocrysts in the basalts and basaltic andesites are totally replaced by smectite with or without hematite and calcite. Primary augite and Fe-Ti oxides are largely unaffected by the zeolite-facies metamorphism. In pervasively altered volcaniclastic rocks and flow breccias, smectitic clay minerals and zeolites pseudomorphically replace most framework grains and fill pore spaces; the development of iron-rich smectites gives these rocks their characteristic green colors. Heulandite, stilbite, and clinoptilolite are the most common zeolites in the volcaniclastic rocks of the map area, indicating that, except for areas near intrusions, metamorphic temperatures did not exceed 180°C (Cho and others, 1987).

Rocks in the gorge of the East Fork Lewis River upstream of Moulton Falls are more altered than those elsewhere in the map area; secondary quartz and calcite occupy amygdules and veins, and calcite extensively replaces plagioclase phenocrysts. Alteration of this type is typical of the outer fringes of areas affected by large intrusions in the western Cascade Range. The intensity of this alteration, as well as the number of small intrusive bodies, increases to the east in the Dole quadrangle (K.A. Howard and R.C. Evarts, unpub. mapping). In

contrast, the isolated intrusion at Yacolt Mountain imposed no discernible contact-metamorphic effects on its host rocks.

NEOGENE FILL OF THE PORTLAND BASIN

The flat to gently southwest-sloping surfaces below 700 ft (215 m) elevation in the southwest part of the Yacolt quadrangle are underlain by deeply weathered basalt-clast conglomerate (Ttf) that stratigraphically overlies a sequence of fine-grained sedimentary rocks (Tsr). Mundorff (1964) and Howard (2002) assigned both rock types to the Troutdale Formation of Hodge (1938). In the Woodland and Ariel quadrangles, Evarts (2004a, b) mapped equivalent conglomeratic deposits as Troutdale Formation but assigned the subjacent fine-grained strata to the Sandy River Mudstone of Trimble (1963) and this usage is followed here.

The Troutdale Formation and Sandy River Mudstone constitute most of the Neogene fill of the Portland Basin (Trimble, 1963; Mundorff, 1964; Swanson and others, 1993). Surface exposures and numerous water-well logs indicate that these Neogene sedimentary rocks were deposited on an eroded bedrock surface of considerable relief. The bedrock surface slopes irregularly westward in the map area and is located near sea level at the southwestern corner of the quadrangle (Swanson and others, 1993). Information extracted from the logs of several dozen water wells reveals a significant depression of the buried bedrock surface in the area bounded roughly by Salmon Creek, Rock Creek, and Battle Ground Lake.

SANDY RIVER MUDSTONE

In the Yacolt quadrangle, clayey siltstone and sandstone beds of the Sandy River Mudstone are exposed only in a few roadcuts north of Salmon Creek but water-well drillers' logs indicate that the formation constitutes most of the Neogene fill in the map area. Several wells near Crawford penetrate more than 120 m of clay and sand, interpreted as Sandy River Mudstone, beneath a thin cover of gravel. Outcrops in areas to the west of the quadrangle show that the formation consists of well-bedded sandstone, siltstone, and mudstone that typically display graded bedding, planar and trough cross-beds, and cut and fill structures indicative of a fluvial depositional setting (Mundorff, 1964; Howard, 2002; Evarts, 2004a, c). Most of the sandy beds are micaceous lithic and arkosic sandstones. Claystone beds, commonly carbonaceous and tuffaceous in part, increase in abundance downsection and a few interbeds of pebbly conglomerate are present locally. The upper contact with the Troutdale Formation is generally abrupt and probably disconformable.

TROUTDALE FORMATION

In the Yacolt quadrangle the Troutdale Formation underlies the elevated surface west of Rock Creek, part of the Troutdale bench of Mundorff (1964), and laps against Paleogene bedrock south of Salmon Creek. Scattered exposures show that the Troutdale Formation of the map area consists of weakly to moderately cemented pebble and cobble conglomerate and scattered lenses of coarse sandstone and grit. Well rounded pebbles and cobbles eroded from the Columbia River Basalt Group are the most abundant constituent of the conglomerate; the remainder includes light-colored granitic and quartzofeldspathic metamorphic rocks, Fe-oxide stained quartzite, and variable proportions of volcanic rocks eroded from the Cascade Range. The interbedded sandstone ranges in composition from basaltic to muscovite-bearing arkosic and quartzose and is lithologically similar to the sandy matrix of the conglomerate. No sandstones composed predominantly of glassy basaltic debris, the so-called vitric sandstones common in the type area of the Troutdale Formation (Trimble, 1963; Swanson and others, 1993), have been recognized, suggesting that the conglomerate in the Yacolt quadrangle is correlative with the older part of the formation mapped in the Columbia River Gorge by Tolan and Beeson (1984). Deep weathering is characteristic of the Troutdale Formation, and in many places only quartzite pebbles remain. The plutonic and micaceous metamorphic rocks are foreign to western Oregon and Washington and must have been transported by the ancestral Columbia River from pre-Tertiary terranes east of the Cascade Range. Sedimentological characteristics of the conglomerate, such as the massive to crudely stratified beds, clast-support, moderate to good sorting, and clast imbrication, are consistent with deposition during flood stage in a gravelly braided river system (Miall, 1977, 1996; Rust, 1978).

The thickness of the Troutdale Formation in the Yacolt quadrangle increases southwestward from less than 10 m near Crawford to about 50 m in the Morgan Creek area owing to both a southward decline in the elevation of the basal contact and to the erosional removal of the upper part of the formation to the north. Quartzite pebbles lie scattered on the surface at elevations of 600–650 ft (180–200 m) east of Rock and Salmon Creeks, suggesting that the distribution of the conglomerate was at one time more extensive and that the surface of the Troutdale bench extended eastward to the southwest flank of Bells Mountain.

QUATERNARY DEPOSITS

VOLCANIC ROCKS

Battle Ground Volcanic Center

One or more flows of fresh, diktytaxitic, olivine-phyric basalt underlie an area of approximately 12 km^2 in the Yacolt and adjacent Battle Ground quadrangles and probably issued from a vent marked by a pair of cinder cones located just outside the map area about 1 km northwest of Battle Ground Lake (Mundorff, 1964; Howard, 2002). A flow of columnar-jointed basalt exposed above the East Fork Lewis River north of the cinder cones yielded an $^{40}Ar/^{39}Ar$ age of 108±21 ka (R.J. Fleck, written commun., 2002). Chemical analyses (table 1; R.C. Evarts, unpub. data) show the Quaternary basalt is more primitive (Mg# = 64) than the Tertiary basalts in the quadrangle, yet has significantly higher concentrations of incompatible elements such as K, Ba, Sr, and Nb.

The circular crater occupied by Battle Ground Lake exhibits the morphology of a maar produced by explosive interactions of basaltic magma with ground water (Williams and McBirney, 1979; Fisher and Schmincke, 1984). Sparse exposures on the heavily forested crater slopes reveal weathered, red-orange ash and fine-grained (≤2 cm) scoria as well as widely scattered quartzite pebbles from the subjacent Troutdale Formation and blocks of basaltic andesite derived from Tertiary volcanic basement. Massive olivine basalt crops out above the south and southwest shores of the lake, however, and the crest of the crater rim in these areas is littered with angular cobbles of nonvesicular basalt. The basalt exposed in the crater wall is petrographically and chemically indistinguishable from that outside the crater and is, within error limits, the same age, 99±57 ka (R.J. Fleck, written commun., 2002). It appears the crater was formed when magma encountered groundwater-saturated sediment beneath the lava flow, generating violent phreatomagmatic eruptions that blasted upward through the flow.

If this interpretation is correct, the eruption that formed the Battle Ground Lake crater is no older than about 100 ka; it may be much younger. The lake is a maximum of 16 m deep, and piston cores show that sediments beneath the lakebed comprise at least 15 m of inorganic silty clay and laminated and nonlaminated organic-rich mud (Barnosky, 1985; Juvigné, 1986). Several beds of silicic tephra within the sequence are attributed to eruptions of Mount St. Helens; the oldest bed belongs to tephra set S of Mullineaux (1996), which erupted about 13,000 years ago. The deepest core encountered coarse sand and gravel, dated at 20,200±400 ^{14}C years B.P., about 15.4–15.2 m below the lakebed (Barnosky, 1985); these sediments were not described but may consist of pyroclastic debris associated with formation of the crater. Thus, the Battle Ground Lake maar may have formed as recently as about 25 ka. If so, it records the most recent volcanic eruption within the Portland Basin (Conrey and others, 1996; Fleck and others, 2002).

Andesite of Lucia Falls Road

An erosional remnant of a young andesite flow (Qalf) adheres to the north valley wall about 25 m above the East Fork Lewis River between Moulton Falls and Lucia Falls. The flow remnant is about 60 m thick and retains an upper vesicular flow top. This light-gray, vesicular, aphyric lava contrasts with nearby dark, dense, and generally porphyritic Oligocene bedrock. No other outcrops of this flow were seen, so its original extent, age, and source are unknown.

GLACIAL AND RELATED DEPOSITS

Drift

Several times during the Pleistocene epoch, icecaps covered the Washington Cascade Range and spawned glaciers that moved down all of the major river valleys. From examinations of glacial deposits near Mount Rainier, Crandell and Miller (1974) inferred four major glacial episodes, some of which have been shown to consist of several lesser advances and retreats (Dethier, 1988). The most widespread glacial deposits in the range constitute the Hayden Creek Drift of Crandell and Miller (1974). Deeply weathered older deposits are locally preserved in the western Cascade foothills in areas beyond the reach of Hayden Creek glaciers. The last major glaciation in western Washington was the late Wisconsinan Fraser glaciation. Deposits of this age in the Cascade Range, named the Evans Creek Drift, are much less extensive than those of the Hayden Creek age (Crandell and Miller, 1974; Crandell, 1987). Widely distributed till and glaciofluvial sediments in the lower Lewis River valley were named the Amboy Drift by Mundorff (1984), who correlated them with the Hayden Creek Drift of the Mount Rainier region on the basis of similar weathering characteristics. Crandell (1987) noted that some of the till in Mundorff's (1984) Amboy Drift, however, was more deeply weathered than typical Hayden Creek Drift and suggested that the Amboy Drift as mapped by Mundorff (1964, 1984) includes some older drift. Evarts (2004b) distinguished these two drifts in the Ariel and Amboy quadrangles, and informally named the older one the drift of Mason Creek.

Highly weathered till that is assigned to the drift of Mason Creek (Qmt) is present above 1400 ft

(425 m) elevation on the southeast flank of Yacolt Mountain. Weathering rinds on aphanitic andesitic clasts in this deposit range from about 3 mm to 12 mm thick. Glacial ice apparently did not cover the mountain completely, as only bedrock is exposed above about 1670 ft (510 m). Cobble gravel with similar weathering characteristics is found on a hill east of Battle Ground Lake. This hill is the eastern terminus of an irregular highland that marks the southern limit of drift (Mundorff, 1964, 1984; Howard, 2002); the highland may be a highly dissected terminal moraine of Mason Creek age.

Till assigned to the Amboy Drift (Qat) forms a thick blanket over most of the terrain north of the East Fork Lewis River, which marks its southern limit. The Amboy Drift is much less weathered than the older drift; weathering rinds on aphanitic andesitic clasts are generally 1 to 2 mm thick. Small patches of the older drift may exist within this unit as mapped, especially west of Yacolt Mountain where clasts with thick weathering rinds were found in a few roadcuts and Mundorff (1984) noted that some till contains more abundant clayey matrix than elsewhere. More than 40 m of stratified sand and gravel (Qao) underlie the broad, flat-bottomed, gently south-sloping Yacolt Basin. These deposits locally overlie Amboy-age till at the basin margins. Clast compositions and weathering characteristics are similar to those of the till, and the sediments are interpreted as glaciofluvial outwash deposited during the retreat of the Lewis River glacier in late Pleistocene time (Mundorff, 1964, 1984).

The numerical ages of the Hayden Creek Drift and older glacial deposits in the Cascade Range are poorly known. Estimates for the Hayden Creek Drift and its local equivalent, the Amboy Drift, range from 60 ka to greater than 300 ka (Crandell and Miller, 1974; Colman and Pierce, 1981; Dethier, 1988; Grigg and Whitlock, 2002; Evarts, 2004b, 2005; Evarts and others, 2003), and it is likely that till mapped as Hayden Creek based on weathering characteristics represents more than one glacial advance. The age of the drift of Mason Creek is even more uncertain. Weathering characteristics of this drift, particularly the thickness of weathering rinds on volcanic clasts, generally resemble those of the Wingate Hill Drift of Crandell and Miller (1974), estimated to be from 300 to 600 k.y. old (Colman and Pierce, 1981; Dethier, 1988). In the Battle Ground quadrangle, till that is probably equivalent to the drift of Mason Creek is overlain by a lava flow of the basalt of Battle Ground that has been dated by the $^{40}Ar/^{39}Ar$ technique as 108±21 ka (Fleck and others, 2002), thus providing a minimum age for this till, although it is likely much older.

Terrace deposits along the East Fork Lewis River

Terraces underlain by fluvial sand and gravel border the East Fork Lewis River for most of the reach below Moulton Falls. On the basis of topographic position and weathering characteristics, terrace deposits of three ages are distinguished. The oldest terrace deposits (Qtd_3) underlie the broad surface at Heisson and scattered terrace fragments between Heisson Road and Lucia Falls. The surfaces of these deposits vary in elevation between 40 and 50 m above river level and record an apparent paleo-stream gradient (about 8.5 m/km) that is slightly greater than that of the modern river (about 6.8 m/km) within the map area. The deposits consist predominantly of bouldery cobble and pebble gravel with clasts of Tertiary volcanic and granitic rocks as large as 2 m across, and are typically capped by several meters of weathered sand and silt. Weathering rinds on aphanitic andesitic clasts are generally 2 to 5 mm thick. The weathering characteristics and distribution of this unit suggest that it is older than the Amboy Drift. It may consist of outwash that accumulated behind the drift of Mason Creek terminal moraine during retreat of the Mason Creek glacier. The only constraint on the age of this terrace comes from a capping bed of weathered ash that was exposed in a shallow excavation west of Heisson. The ash is mineralogically equivalent to tephras erupted from the Mount St. Helens volcanic center prior to 35 ka (Mullineaux, 1996), and it could be as old as 270 ka (Evarts and others, 2003; Evarts, 2004b).

A lower and hence younger terrace deposit (Qtd_2) with tread elevations between 25 and 30 m above East Fork Lewis River extends along the south side of the river for a distance of 2.5 km upstream from Lucia Falls. Railroad cuts at Lucia show that the upper part of this unit consists of poorly sorted bouldery cobble gravel with well rounded to subrounded clasts as large as 1 m across in a matrix of coarse rusty sand. Weathering rinds on the volcanic clasts are 1 to 2 mm thick, similar to those in the Amboy Drift. Assuming a stream profile comparable to that defined by the older terrace set (Qtd_3), the surface of this unit grades upstream to the Amboy-age outwash (Qao) south of Yacolt, implying that the terrace formed by unit Qtd_2 is probably the distal remnant of a valley train formed during the late Pleistocene retreat of the Amboy-age glacier northward into the Lewis River valley.

Both of the older terrace deposits (Qtd_3 and Qtd_2) shown on this map were mapped as drift by Mundorff (1964), but he clearly considered them to form the upper end of an alluvial fan, centered northeast of Battle Ground, which he interpreted as the distal equivalent of the outwash plain south of Yacolt. Similarly, Howard (2002) mapped deposits

contiguous with the oldest terrace deposits (Qtd_3) at the west edge of the Yacolt quadrangle partly as drift and partly as alluvial-fan deposits, which he suggested might be outwash. However, only the intermediate-age terrace deposits (Qtd_2) in the map area grade to the Amboy-age fill at Yacolt, and it is unclear which, if any, of the deposits mapped by Howard (2002) downstream are correlative. The oldest terrace deposits (Qtd_3), and probably the alluvial fan deposits that Mundorff (1964; 1984) and Howard (2002) mapped northeast of Battle Ground, are more likely related to the drift of Mason Creek, which neither author differentiated from the younger drift.

The youngest and best preserved terrace deposits (Qtd_1) are typically about 10 m thick and have surface elevations 10 to 15 m above river level. Inset against the older terrace deposits, the younger deposits rest on bedrock along both banks of the East Fork Lewis River and underlie a large area, on which abandoned channels are still visible, north of the river between Lucia Falls and the bridge north of Heisson. These deposits consist largely of clast-supported gravel and minor coarse sand. They are weakly indurated, crudely stratified, and poorly sorted, and contain clasts of Tertiary volcanic and granitic rocks as large as 2 m across in a sandy matrix. At several localities the basal bed is a distinctive diamict that contains angular and rounded clasts as large as 25 cm in a light brown, compact, silty matrix. Abundant angular clasts of platy aphyric basaltic andesite are a conspicuous component of the diamicton. These clasts closely resemble a lava flow exposed in the headwall scarp of a landslide north of the railroad bridge between Lucia Falls and Moulton Falls, suggesting that the diamict, which has not been found upstream from the landslide, may be a debris flow triggered by the movement of slide debris into the river. The age of the diamict and overlying gravel are unknown, but here and to the west (Howard, 2002) they occupy a channel incised into the Amboy Drift and the basalt of Battle Ground, and the absence of significant weathering rinds on volcanic clasts indicates the gravel is unlikely to be much older than 20 ka (Colman and Pierce, 1981). These weathering characteristics are similar to those described for the Evans Creek Drift (Crandell and Miller, 1974), and the gravel may be distal outwash from an Evans Creek-age glacier in the headwaters of the East Fork Lewis River. The youngest terrace deposits in the Yacolt quadrangle are equivalent, in part, to sediments mapped as terrace deposits (Qt) and older alluvium (Qoa) by Howard (2002) in adjacent Battle Ground quadrangle.

Cataclysmic-flood deposits

During the last glacial maximum in late Pleistocene time, an ice dam at Pleistocene Lake Missoula in western Montana failed repeatedly, each collapse generating enormous floods, commonly referred to as the Missoula floods, that coursed down the Columbia River and into the Portland Basin (Bretz, 1925, 1959; Bretz and others, 1956; Trimble, 1963; Baker and Bunker, 1985; Waitt, 1985, 1994, 1996; O'Connor and Baker, 1992; Benito and O'Connor, 2003). The sediment-laden floodwaters were hydraulically dammed by the relatively narrow constriction of the Columbia River valley at the north end of the Portland Basin, causing temporary ponding in the Portland Basin and tributary valleys to elevations as high as 400 ft (120 m). Radiocarbon ages, paleomagnetic measurements, and tephrochronologic data indicate that these floods occurred chiefly between about 17,000 and 13,000 ^{14}C years B.P. (Waitt, 1985, 1994; Atwater, 1986; Clague and others, 2003), although evidence is accumulating for episodes of cataclysmic flooding earlier in the Quaternary (McDonald and Busacca, 1988; Zuffa and others, 2000; Bjornstad and others, 2001).

During each flood event, the suspended load of fine sand and silt settled out of the temporarily ponded floodwaters. Perhaps as many as 100 such floods (Waitt, 1994) collectively built up deposits of laminated micaceous silts as thick as 30 m in the northern part of the Portland Basin. These slackwater silts underlie the low-relief terrain below about 350 ft (110 m) elevation near the southwest corner of the map area. They are rarely exposed, however, and their thickness (less than 10 m) and distribution are inferred largely from water-well logs.

LANDSLIDE, TALUS, AND ALLUVIAL DEPOSITS

Landslide deposits (Qls) are widespread in the Yacolt quadrangle. Most result from failure of weathered, clay-rich, Paleogene volcaniclastic rocks (Tvs, Tvb, and unmapped sedimentary interbeds within Tbem). Younger, poorly lithified deposits of the Troutdale Formation and Sandy River Mudstone as well as Quaternary fluvial sand and gravel are also susceptible to sliding, especially on steeper slopes along streams. Only the larger landslides are shown on this map; many areas underlain by unconsolidated Quaternary units contain small slumps and debris-flow deposits too small to portray at 1:24,000 scale.

Deposits of talus, scree, and colluvium (Qt) have accumulated beneath many steep slopes and cliffs in the Yacolt quadrangle, most notably below the steep north flank of Bells Mountain. Unconsolidated alluvium (Qa) includes local accumulations of sand and gravel along low-gradient reaches of Salmon and Rock Creeks and ephemeral gravel bars in the East Fork Lewis River.

STRUCTURAL FEATURES

Structural attitudes of Paleogene strata north and northeast of the map area delineate a set of large-amplitude, south- to southeast-plunging folds that are believed to have developed in late early Miocene time (Evarts and Swanson, 1994). These folds die out southward (Phillips, 1987), and sparse bedding readings and the distribution of individual volcaniclastic beds and lava flows show that the Oligocene strata of the Yacolt quadrangle are nearly flat lying, with very low (less than 5°) dips to the south, southwest, and west.

The Yacolt quadrangle lies along the eastern margin of the Portland Basin (fig. 1B), where Neogene basin-fill deposits onlap Paleogene volcanic bedrock. Although this margin is probably tectonic in origin (Yelin and Patton, 1991; Beeson and others, 1989; Blakely and others, 1995), compelling evidence for the existence of faults in the map area is sparse owing to limited outcrop. However, several faults have been inferred from apparent discontinuities in stratigraphic units, from topographic lineaments, or from areas of hydrothermally altered rock. Most appear to be northwest- to north-northwest-striking high-angle normal, strike-slip, or oblique-slip faults that roughly parallel the basin margin.

Mundorff (1964) recognized that the flat-bottomed elongate valley occupied by Yacolt is probably bounded by a fault on its west side. I interpret the valley as a transtensional graben bounded by two sets of oblique-slip faults that, to the north, appear to exhibit dextral offsets (Evarts, 2005). Mundorff (1964) projected a fault strand southeastward along the East Fork Lewis River upstream from the mouth of Big Tree Creek; excellent riverbed outcrops, however, reveal no evidence of disruption in this area.

Another fault zone, also mapped by Mundorff (1964), strikes northwest from Salmon Falls to the confluence of Salmon and Rock Creeks and continues to the north-northwest along Rock Creek. The fault changes character along strike. Minor dextral offset of Oligocene lava flows is present near Salmon Falls, but the segment along Rock Creek, which is locally marked by hydrothermally altered bedrock, is primarily vertical. Water wells west of the fault between Pantoski Road and Salmon Creek penetrate Paleogene bedrock at elevations at least 50 m lower than the Paleogene bedrock surface to the east. Near Crawford, wells bottom in Sandy River Mudstone (Tsr) at elevations as low as 150 ft (45 m), nearly 150 m below bedrock exposed at 630 ft (190 m) on the hill to the northeast. East of Crawford, the fault splays into three strands, the westernmost of which continues into the Battle Ground quadrangle (Howard, 2002). A fault in the valley of Salmon Creek west of the mouth of Rock Creek drops Neogene sedimentary rocks on the north against Paleogene bedrock. This structure also continues west into the Battle Ground quadrangle (Howard, 2002).

The age of the faulting in the Yacolt quadrangle is poorly constrained and it may well have occurred intermittently throughout much of late Tertiary time. The low-temperature hydrothermal alteration in Rock Creek presumably records reaction with geothermal fluids moving along the fault plane, which suggests this structure existed before magmatic and associated hydrothermal activity in the southern Washington Cascade Range declined precipitously near 17 Ma (Evarts and Swanson, 1994). If so, the fault was apparently reactivated because it and the east-west fault along Salmon Creek juxtapose late Miocene Sandy River Mudstone against Paleogene bedrock. These normal faults may have been active throughout late Miocene time as the Sandy River Mudstone accumulated in the subsiding Portland Basin (Trimble, 1963; Swanson and others, 1993). The fault along Rock Creek may have offset the overlying Troutdale Formation as well, but this is not required by the field relations. Most movement on these structures probably ended in late Miocene or Pliocene time, although Howard and others (2000) suggest possible Holocene activity on the fault along Salmon Creek west of the map area. The fault zones expressed in the linear, scarp-like flanks of Yacolt valley may be relatively young and possibly Quaternary in age, but glacial scouring has probably enhanced the steepness of the valley walls, and no scarps have been noted on the surface of the late Pleistocene outwash fill. Nevertheless, the north-northwest-striking fault zones are parallel to the right-lateral St. Helens Seismic Zone of Weaver and others (1987) beneath Mount St. Helens and appear to be appropriately oriented for dextral shear in the modern regional stress field (Pezzopane and Weldon, 1993; Wells and others, 1998; Miller and others, 2001).

GEOLOGIC EVOLUTION

The Oligocene volcanic bedrock of the Yacolt quadrangle is compositionally restricted in comparison to that of most areas in the southern Washington Cascade Range (Evarts and others, 1987; Evarts and Swanson, 1994; Evarts, 2004a, b; 2005). Most lava flows in the map area belong to a chemically coherent suite of tholeiitic basalt and basaltic andesite herein named the basaltic andesite of Elkhorn Mountain. These flows were probably emplaced on the middle to lower flanks of large shield volcano during an eruptive episode lasting less than 1 m.y. Neither dikes nor intense hydrothermal

alteration are present in the map area, indicating that the vent for this volcano is located outside the quadrangle, probably to the east or southeast, where clastic rocks are rare. To the northwest, between Bells Mountain and the East Fork Lewis River, interbedding of the flows with debris-flow deposits and epiclastic volcaniclastic rocks suggests depositional settings on or near the lower flank of a volcanic edifice (Williams and McBirney, 1979; Vessel and Davies, 1981; Cas and Wright, 1987; Orton, 1996).

The stock at Yacolt Mountain is a calc-alkaline quartz diorite compositionally distinct from any extrusive rock in the map area. It had not been dated, but similar intrusions in the southern Washington Cascade Range are generally no younger than early Miocene.

Field relations and radiometric age determinations in the Yacolt and adjacent quadrangles suggest that this part of the Cascade volcanic arc experienced an episode of diminished volcanic activity and consequent erosion in middle Oligocene time, between 32 and 27 Ma. To the north and northeast, arc strata were deformed during an early to middle Miocene episode of uplift, folding, and erosion (Evarts and Swanson, 1994). This deformation dies out southward, however, as reflected in the gentle dips evident in the Yacolt quadrangle.

Development of the Portland Basin apparently began at about the same time as the Miocene regional folding event (Beeson and others,1989; Beeson and Tolan, 1990). Fine-grained nonmarine sediments of the Sandy River Mudstone, which record deposition in low-energy fluvial and lacustrine environments along an ancestral Columbia River, began to accumulate in the incipient Portland Basin and similar settings to the south and west (Van Atta and Kelty, 1985; Beeson and others, 1989; Tolan and Beeson, 1999). The absence of coarse-grained volcaniclastic debris indicates that the middle Miocene Cascade arc of southern Washington and northern Oregon was topographically subdued and volcanically quiescent compared to earlier times. The north-northwest- and east-northeast-trending normal faults in the western Yacolt quadrangle are interpreted as basin-bounding structures that were active during Sandy River time.

In the northern Portland Basin, the fine-grained basin-fill strata of the Sandy River Mudstone are disconformably overlain by conglomeratic beds of the Troutdale Formation (Trimble, 1963; Mundorff, 1964; Swanson and others, 1993; Evarts, 2004a, c). Clasts eroded from flows of the Miocene Columbia River Basalt Group constitute the predominant component of these gravelly beds, but they also contain clasts of quartzite, granite, and metamorphic rocks derived from pre-Tertiary terranes east of the Cascade Range. Superposition of the Troutdale Formation on the Sandy River Mudstone evidently records the northward progradation of a gravelly, braided, alluvial plain across the Portland Basin during late Miocene or early Pliocene time. This pronounced change in the Columbia River sedimentary regime may record regional uplift to the east and initial incision of the Columbia River Gorge.

The southwestward tilt of the surface of the Troutdale Formation indicates that the Portland Basin continued to develop into Pliocene time. If Troutdale Formation sediments were deposited near sea level, as suggested by Beeson and Tolan (1990), then their present position at elevations greater than 600 ft (180 m) in the map area implies that uplift of the Cascade Range occurred concurrently with the later stages of basin-floor subsidence. This uplift caused the Columbia River to incise its floodplain and remove the late Miocene to early Pliocene gravel from much of the northern Portland Basin, leaving remnants preserved only on the uplifted basin flanks. Continued regional uplift may explain the changes in apparent stream gradient recorded by Pleistocene terraces along the East Fork Lewis River.

The Quaternary geologic history recorded in the Yacolt quadrangle reflects the dominant influence of Pleistocene glaciation (Mundorff, 1984). Several times during the Pleistocene, mountain glaciers formed high in the southern Washington Cascade Range, and large piedmont glaciers issuing from the Lewis River valley spread southward into the map area. All of the terrain north of the East Fork Lewis River except for the summit of Yacolt Mountain was buried in ice. Much of the evidence for earlier glacial advances was erased by the glaciation that deposited the Amboy Drift. However, deeply weathered and dissected pre-Amboy glacial deposits, the drift of Mason Creek, are found beyond the limits of the Amboy Drift to the west and northwest of the map area (Evarts, 2004b), and deposits of similar character underlies hills south of Heisson that may be the remains of a Mason Creek-age terminal moraine. Heisson sits on a terrace surface underlain by deeply weathered fluvial deposits, which may be outwash that accumulated behind the moraine as the Mason Creek glacier melted. This terrace is capped by ash erupted from Mount St. Helens that may be as old as 270 ka, thus the Mason Creek Drift may be older than MIS 8 (245–300? ka; Martinson and others, 1987). The Amboy Drift, the local equivalent of the widespread Hayden Creek Drift (Crandell and Miller, 1974), probably includes deposits of more than one glacial pulse during the Hayden Creek Stade, with the maximum advance occurring at about 270 ka (Evarts and others, 2003; Evarts, 2004b), that is, during MIS 8. In the Yacolt quadrangle, the Amboy-age glacier(s) extended to the East Fork Lewis River but

did not cross it as the older Mason Creek-age glacier(s) did. The most recent glaciation in the Cascade Range, which culminated about 17 ka (Barnosky, 1984), was considerably less extensive than the Hayden Creek/Amboy advance (Crandell and Miller, 1974). The only deposits in the map area possibly related to this event are the lowest terraces along the East Fork Lewis River.

As noted by Mundorff (1964, 1984), the presence of Pleistocene glaciers caused considerable derangement of drainage patterns as proglacial streams adjusted to the changing position of ice

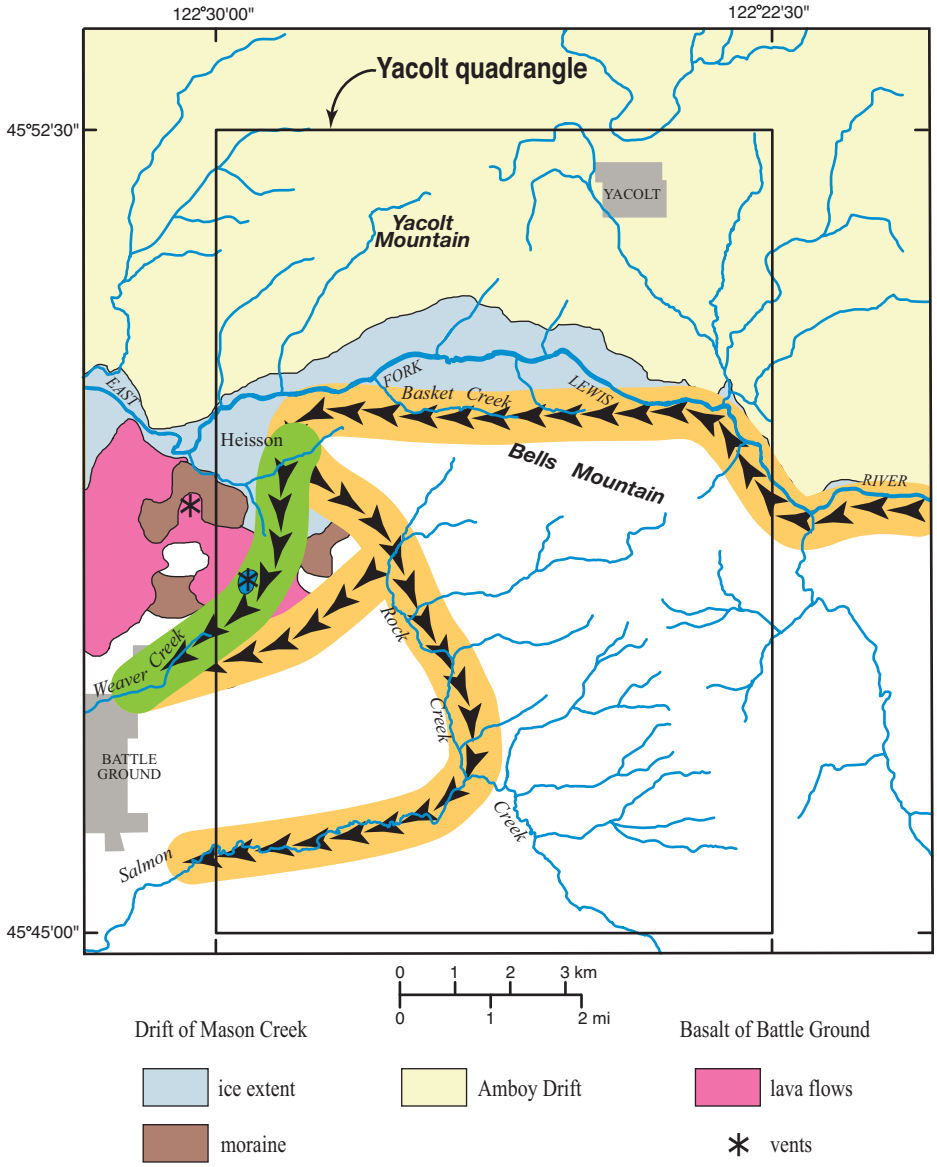

Figure 5. Modern drainage in Yacolt 7.5' quadrangle and vicinity and flow paths (marked by arrows) of ancestral East Fork Lewis River at height of (orange) and following (green) the Middle Pleistocene(?) glaciation that deposited the drift of Mason Creek, as inferred from the distribution of drift and locations of benches with exceptionally thin cover of soil or alluvium. Location of flow path along the north and east flanks of Bells Mountain marks terminus of the Mason Creek-age glacier. Flow path running south from Heisson through gap in moraine is possible route of postglacial East Fork. Basalt of Battle Ground is postglacial volcanic center constructed on top of Mason Creek end moraine.

margins. When the ice reached its maximum extent, during Mason Creek time, it shunted the East Fork Lewis River southward. The glacier-marginal course of the river is recorded by a series of benches along the north and northwest flanks of Bells Mountain (Mundorff, 1964). The elevations of these benches decrease from about 850 to 950 ft (260 to 290 m) above Moulton Falls to about 540 to 740 ft (165 m to 225 m) in lower Basket Creek. A few well rounded pebbles and cobbles lie scattered on top of the benches and one deeply weathered outcrop of poorly sorted gravel was seen on the large sloping bench about 1 km southeast of Lucia. In most places, however, the benches are bedrock surfaces mantled by a thin layer of silt but free of coarse sediment. A series of similar low-relief surfaces, mostly lacking a cover of alluvial sediment or thick soil, extends from east of Heisson southeastward to the mouth of Rock Creek, which, like Basket Creek, appears to be an underfit stream. These surfaces may mark the course of the East Fork Lewis River along the south margin of the Mason Creek-age glacier; the small fan of gravelly alluvium (Qa) at the east end of the moraine may have been deposited by this stream. Ice blocked the valley at Heisson, forcing the river to spill southward along flow paths marked by Rock, Salmon, and Weaver Creeks (fig. 5). The ice later retreated northward across the East Fork Lewis but still filled the valley of Yacolt Creek. The East Fork, laden with sediment from melting glaciers in its headwaters, deposited sand and gravel behind the Mason Creek moraine and built a narrow outwash plain, the remnants of which grade upriver from Heisson to an elevation about 30 m higher than the floor of the Yacolt Creek valley.

Mundorff (1984) postulated that the East Fork Lewis River flowed northwest through the valley occupied by Yacolt and into the Cedar Creek valley prior to the Amboy glaciation. However, the deep valley of the East Fork, more than 380 m deep between Yacolt Mountain and Bells Mountain, must have been cut by an ancestral East Fork Lewis River over a long period of time. It seems more likely that pre-glacial Cedar Creek once flowed southward to join the East Fork Lewis at the south end of the fault-bounded Yacolt valley. The slightly lower elevation of the bedrock floor at the north end of the valley cited by Mundorff (1984) probably reflects overdeepening by glacial abrasion rather than stream incision. When ice occupied the valley during Amboy time, Cedar Creek was temporarily diverted along the southwestern margin of the glacier and carved a narrow north-south valley now perched near the northeast corner of the map area. As the Amboy glacier retreated, a south-sloping fan of outwash filled the valley and extended down the East Fork. Post-glacial headward erosion by lower Cedar Creek south of Amboy eventually captured the upper reach of the creek, resulting in the curiously opposed courses of Cedar and Yacolt Creeks within about 400 m of each other north of Yacolt.

Young volcanic rocks in the Yacolt quadrangle erupted from the northernmost vents of the Late Pliocene and Quaternary Boring Volcanic Field of the Portland Basin (Allen, 1975; Conrey and others, 1996; Fleck and others, 2002). At about 100 ka, olivine-rich mafic lava flows erupted from a vent located just west of the map area and partly buried the drift of Mason Creek end moraine. Before this time, the East Fork Lewis River may have flowed through a breach in the Mason Creek-age moraine south of Heisson, along the course of modern Weaver Creek (fig. 5), and it attained its present course when basalt flows blocked that channel. Later, perhaps as recently as 25,000 to 30,000 years ago, a phreatomagmatic eruption blasted through one of the flows to form a maar now occupied by Battle Ground Lake. The remnant of an andesite flow crops out in the East Fork Lewis River valley east of Lucia Falls. Neither the source of the flow nor its age are known, although it is overlain by Amboy Drift. Its base is about 30 m above the river, suggesting considerable incision since its emplacement.

The most recent major geologic events to affect the Yacolt quadrangle were the cataclysmic Missoula floods, which inundated the Portland Basin and draped a layer of slack-water silt over low-elevation terrain along Salmon Creek.

GEOLOGIC RESOURCES

Known geologic resources available in the Yacolt quadrangle are limited to nonmetallic industrial materials, chiefly aggregate for road construction and similar purposes. Paleogene volcanic bedrock has locally been quarried for crushed aggregate used primarily as base and surface layers for logging roads. Sand and gravel deposits have been exploited along the East Fork Lewis River downstream from the quadrangle (Norman and others, 1998) but are sparse within the bedrock-floored reach of the river in the map area. According to Huntting (1949), clay for brickmaking was extracted from a pit near Crawford, most likely from the Sandy River Mudstone or deeply weathered Troutdale Formation.

REFERENCES CITED

Allen, J.E., 1975, Volcanoes of the Portland area: Ore Bin, v. 37, p. 145–157.

Atwater, B.F., 1986, Pleistocene glacial-lake deposits of the Sanpoil River Valley, northeastern Washington: U.S. Geological Survey Bulletin

1661, 39 p.
Baker, V.R., and Bunker, R.C., 1985, Cataclysmic late Pleistocene flooding from glacial Lake Missoula—a review: Quaternary Science Reviews, v. 4, p. 1–41.
Balsillie, J.H., and Benson, G.T., 1971, Evidence for the Portland Hills Fault: The Ore Bin, v. 33, p. 109–118.
Barnosky, C.W., 1984, Late Pleistocene and early Holocene environmental history of southwestern Washington State, U.S.A.: Canadian Journal of Earth Sciences, v. 21, p. 619–629.
Barnosky, C.W., 1985, Late Quaternary vegetation near Battle Ground Lake, southern Puget Trough, Washington: Geological Society of America Bulletin, v. 96, p. 263–271.
Beeson, M.H., Fecht, K.R., Reidel, S.P., and Tolan, T.L., 1985, Regional correlations within the Frenchman Springs Member of the Columbia River Basalt Group—new insights into the middle Miocene tectonics of northwestern Oregon: Oregon Geology, v. 47, p. 87–96.
Beeson, M.H., and Tolan, T.L., 1990, The Columbia River Basalt Group in the Cascade Range; a middle Miocene reference datum for structural analysis: Journal of Geophysical Research, v. 96, p. 19,547–19,559.
Beeson, M.H., Tolan, T.L., and Anderson, J.L., 1989, The Columbia River Basalt Group in western Oregon; geologic structures and other factors that controlled flow emplacement patterns, *in* Reidel, S.P., and Hooper, P.R, eds., Volcanism and tectonism in the Columbia River flood-basalt province: Geologic Society of America Special Paper 239, p. 223–246.
Benito, G., and O'Connor, J.E., 2003, Number and size of last-glacial Missoula floods in the Columbia River valley between the Pasco Basin, Washington and Portland, Oregon: Geological Society of America Bulletin, v. 115, p. 624–638.
Berggren, W.A., Kent, D.V., Swisher, C., III, Aubry, M.-P., 1995, A revised Cenozoic geochronology and chronostratigraphy, *in* Berggren, W.A., Kent, D.V., Aubry, M.-P., and Hardenbol, J., eds., Geochronology, time scales and global stratigraphic correlation: Society of Economic Paleontologists and Mineralogists Special Publication 54, p. 129–212.
Bjornstad, B.N., Fecht, K.R., and Pluhar, C.J., 2001, Long history of pre-Wisconsin, Ice Age cataclysmic floods—evidence from southeastern Washington State: Journal of Geology, v. 109, p. 695–713.
Blakely, R.J., Wells, R.E., Yelin, T.S., Madin, I.P., and Beeson, M.H., 1995, Tectonic setting of the Portland-Vancouver area, Oregon and Washington—constraints from low-altitude aeromagnetic data: Geological Society of America Bulletin, v. 107, p. 1051–1062.
Bott, J.D.J., and Wong, I.G., 1993, Historical earthquakes in and around Portland, Oregon: Oregon Geology, v. 55, p. 116–122.
Bretz, J H., 1925, The Spokane flood beyond the Channeled Scablands: Journal of Geology, v. 33, p. 97–115, p. 236–259.
Bretz, J H., 1959, Washington's Channeled Scabland: Washington Division of Mines and Geology Bulletin 45, 55. p.
Bretz, J H., Smith, H.T.U., and Neff, G.E., 1956, Channeled Scabland of Washington—new data and interpretations: Geological Society of America Bulletin, v. 67, p. 957–1049.
Cas, R.A.F., and Wright, J.V., 1987, Volcanic successions—modern and ancient: London, Allen and Unwin, 528 p.
Cho, M., Maruyama, S., and Liou, J.G., 1987, An experimental investigation of heulandite-laumontite equilibrium at 1000 to 2000 bar P_{fluid}: Contributions to Mineralogy and Petrology, v. 97, p. 43–50.
Clague, J.J., Barendregt, R. Enkin, R.J., and Foit, F.F., Jr., 2003, Paleomagnetic and tephra evidence for tens of Missoula floods in southern Washington: Geology, v. 31, p. 247–250.
Colman, S.M., and Pierce, K.L., 1981, Weathering rinds on andesitic and basaltic stones as a Quaternary age indicator, western United States: U.S. Geological Survey Professional Paper 1210, 56 p.
Conrey, R.M., Uto, K., Uchiumi, S., Beeson, M.H., Madin, I.P., Tolan, T.L., Swanson, D.A., 1996, Potassium-argon ages of Boring Lava, northwest Oregon and southwest Washington: Isochron West, no. 63, p. 3–9.
Crandell, D.R., 1987, Deposits of pre-1980 pyroclastic flows and lahars from Mount St. Helens, Washington: U.S. Geological Survey Professional Paper 1444, 91 p.
Crandell, D.R., and Miller, R.D., 1974, Quaternary stratigraphy and extent of glaciation in the Mount Rainier region, Washington: U.S. Geological Survey Professional Paper 847, 59 p.
Dethier, D.P., 1988, The soil chronosequence along the Cowlitz River, Washington: U.S. Geological Survey Bulletin 1590-F, p. F1–F47.
Evarts, R.C., 2001, Geologic map of the Silver Lake quadrangle, Cowlitz County, Washington: U.S. Geological Survey Miscellaneous Field Studies Map MF-2371, scale 1:24,000, with 37-p. pamphlet [http://geopubs.wr.usgs.gov/map-mf/mf2371/].
Evarts, R.C., 2002, Geologic map of the Deer Island quadrangle, Cowlitz County, Washington: U.S.

Geological Survey Miscellaneous Field Studies Map MF-2392, scale 1:24,000, with 33-p. pamphlet [http://geopubs.wr.usgs.gov/map-mf/mf2392/].

Evarts, R.C., 2004a, Geologic map of the Woodland quadrangle, Cowlitz and Clark Counties, Washington: U.S. Geological Survey Scientific Investigations Map 2827, scale 1:24,000, with 38-p. pamphlet [http://pubs.usgs.gov/sim/2004/2827].

Evarts, R.C., 2004b, Geologic map of the Ariel quadrangle, Clark and Cowlitz Counties, Washington: U.S. Geological Survey Scientific Investigations Map 2826, scale 1:24,000, with 35-p. pamphlet [http://pubs.usgs.gov/sim/2004/2826].

Evarts, R.C., 2004c, Geologic map of the Ridgefield quadrangle, Clark and Cowlitz Counties, Washington: U.S. Geological Survey Scientific Investigations Map 2844, scale 1:24,000, with 21-p. pamphlet [http://pubs.usgs.gov/sim/2004/2844].

Evarts, R.C., 2005, Geologic map of the Amboy quadrangle, Clark and Cowlitz Counties, Washington: U.S. Geological Survey Scientific Investigations Map 2885, scale 1:24,000, with 25-p. pamphlet [http://pubs.usgs.gov/sim/2005/2885].

Evarts, R.C., and Ashley, R.P., 1990a, Preliminary geologic map of the Cougar quadrangle, Cowlitz and Clark Counties, Washington: U.S. Geological Survey Open-File Report 90-631, scale 1:24,000, with 40-p. pamphlet.

Evarts, R.C., and Ashley, R.P., 1990b, Preliminary geologic map of the Goat Mountain quadrangle, Cowlitz County, Washington: U.S. Geological Survey Open-File Report 90-632, scale 1:24,000, with 47-p. pamphlet.

Evarts, R.C., and Ashley, R.P., 1991, Preliminary geologic map of the Lakeview Peak quadrangle, Cowlitz County, Washington: U.S. Geological Survey Open-File Report 91-289, scale 1:24,000, with 35-p. pamphlet.

Evarts, R.C., and Ashley, R.P., 1992, Preliminary geologic map of the Elk Mountain quadrangle, Cowlitz County, Washington: U.S. Geological Survey Open-File Report 92-362, scale 1:24,000, with 44-p. pamphlet.

Evarts, R.C., Ashley, R.P., and Smith, J.G., 1987, Geology of the Mount St. Helens area—record of discontinuous volcanic and plutonic activity in the Cascade arc of southern Washington: Journal of Geophysical Research, v. 92, p. 10,155–10,169.

Evarts, R.C., and Bishop, K.R., 1994, Chemical data for Tertiary volcanic and intrusive rocks of the Spirit Lake 15-minute quadrangle, southern Washington Cascade Range: U.S. Geological Survey Open-File Report 93-686, 24 p.

Evarts, R.C., Clynne, M.A., Fleck, R.J., Lanphere, M.A., Calvert, A.T., and Sarna-Wojcicki, A.M., 2003, The antiquity of Mount St. Helens and age of the Hayden Creek Drift [abs.]: Geological Society of America Abstracts with program, v. 35, no. 6, p. 80.

Evarts, R.C., and Swanson, D.A., 1994, Geologic transect across the Tertiary Cascade Range, southern Washington, *in* Swanson, D.A., Haugerud, R.A., eds., Geologic field trips in the Pacific Northwest, 1994 Geological Society of America Meeting: Seattle, University of Washington Department of Geological Sciences, v. 2, p. 2H1–2H31.

Fisher, R.V., and Schmincke, H.-U., 1984, Pyroclastic rocks: New York, Springer-Verlag, 472 p.

Fiske, R.S., Hopson, C.A., and Waters, A.C., 1963, Geology of Mount Rainier National Park, Washington: U.S. Geological Survey Professional Paper 444, 93 p.

Fleck, R.J., Evarts, R.C., Hagstrum, J.T., and Valentine, M.J., 2002, The Boring Volcanic Field of the Portland, Oregon area—geochronology and neotectonic significance: Geological Society of America Abstracts with Program, v. 33, no. 5, p. 33–34.

Gill, J.B., 1981, Orogenic andesites and plate tectonics: New York, Springer-Verlag, 390 p.

Grigg, L.D., and Whitlock, C., 2002, Patterns and causes of millennial-scale climate change in the Pacific Northwest during Marine Isotope stages 2 and 3: Quaternary Science Reviews, v. 21, p. 2067–2083.

Hodge, E.T., 1938, Geology of the lower Columbia River: Geological Society of America Bulletin, v. 49, p. 836–929.

Howard, K.A., 2002, Geologic map of the Battle Ground 7.5-minute quadrangle, Clark County, Washington: U.S. Geological Survey Miscellaneous Field Studies Map MF-2395, scale 1:24,000, with 18-p. pamphlet [http://pubs.usgs.gov/mf/2002/2395/].

Howard, K.A., Blakely, R.J., and Haugerud, R.A., 2000, Neotectonics of the Portland basin—possible uplift and offset of latest Pleistocene Missoula flood deposits near Battle Ground, Washington [abs.]: Geological Society of America Abstracts with Program, v. 32, no. 6, p. A-20.

Huntting, M.T., 1949, Directory of Washington mining operations, 1949: Washington Division of Mines Information Circular 17, 62 p.

Johnson, D.M., Hooper, P.R., and Conrey, R.M., 1999, XRF analysis of rocks and minerals for major and trace elements on a single low

dilution Li-tetraborate fused bead: Advances in X-ray Analysis, v. 41, p. 843–867.

Juvigné, E.H., 1986, Late-Quaternary sediments at Battle Ground Lake, southern Puget Trough, Washington: Northwest Science, v. 60, p. 210–217.

Le Maitre, R.W., 2002, Igneous rocks—a classification and glossary of terms (2d ed.): Cambridge University Press, 236 p.

Liberty, L.M., Hemphill-Haley, M.A., and Madin, I.P., 2003, The Portland Hills Fault—uncovering a hidden fault in Portland, Oregon using high-resolution geophysical methods: Tectonophysics, v. 368, p. 89–103.

Madin, I.P., and Wang, Z., 1999, Relative earthquake hazard maps for selected urban areas in western Oregon—Dallas, Hood River, McMinnville-Dayton-Lafayette, Monmouth-Independence, Newberg-Dundee, Saint Helens-Columbia City-Scappoose, Sandy, Sheridan-Williamina: Oregon Department of Geology and Mineral Industries Interpretative Map Series IMS-7, scale 1:24,000, with 24-p. pamphlet.

Martinson, D.G., Pisias, N.G., Hayes, J.D., Imbrie, J., Moore, T.C., Jr., and Shackleton, N.J., 1987, Age dating and orbital theory of the ice ages—development of a high-resolution 0 to 300,000-year chronostratigraphy: Quaternary Research, v. 27, p. 1–29.

McDonald, E.V., and Busacca, A.J., 1988, Record of pre-late Wisconsin giant floods in the Channeled Scabland interpreted from loess deposits: Geology, v. 16, p. 728–731.

Miall, A.D., 1977, A review of the braided river depositional environment: Earth-Science Reviews, v. 13, p. 1–62.

Miall, A.D., 1996, The geology of fluvial deposits—sedimentary facies, basin analysis, and petroleum geology: Berlin, Springer, 582 p.

Miller, M.M., Johnson, D.J., Rubin, C.M., Dragert, H., Wang, K., Qamar, A., and Goldfinger, C., 2001, GPS-determination of along-strike variation in Cascadia margin kinematics—implications for relative plate motion, subduction zone coupling, and permanent deformation: Tectonics, v. 20, p. 161–171.

Miyashiro, A., 1974, Volcanic rocks series in island arcs and active continental margins: American Journal of Science, v. 274, p. 321–355.

Mullineaux, D.R., 1996, Pre-1980 tephra-fall deposits erupted from Mount St. Helens: U.S. Geological Survey Professional Paper 1563, 99 p.

Mundorff, M.J., 1964, Geology and ground-water conditions of Clark County, Washington, with a description of a major alluvial aquifer along the Columbia River: U.S. Geological Survey Water-Supply Paper 1600, 268 p., scale 1:48,000.

Mundorff, M.J., 1984, Glaciation in the lower Lewis River basin, southwestern Cascade Range, Washington: Northwest Science, v. 58, p. 269–281.

Norman, D.K., Cederholm, C.J., and Lingley, W.S., Jr., 1998, Flood plains, salmon habitat, and sand and gravel mining: Washington Geology, v. 26, no. 2/3, p. 3–20.

O'Connor, J.E., and Baker, V.R., 1992, Magnitudes and implications of peak discharges from glacial Lake Missoula: Geological Society of America Bulletin, v. 104, p. 267–279.

Orton, G.J., 1996, Volcanic environments, *in* Reading, H.G., ed., Sedimentary environments—processes, facies and stratigraphy (3d ed.): Oxford, Blackwell Science, Ltd., p. 485–567.

Pezzopane, S.K., and Weldon, R.J., II, 1993, Tectonic role of active faulting in central Oregon: Tectonics, v. 12, p. 1140–1169.

Phillips, W.M., 1987, comp., Geologic map of the Vancouver quadrangle, Washington: Washington Division of Geology and Earth Resources Open-File Report 87-10, scale 1:100,000, with 27-p. pamphlet.

Roberts, A.E., 1958, Geology and coal resources of the Toledo-Castle Rock district, Cowlitz and Lewis Counties, Washington: U.S. Geological Survey Bulletin 1062, 71 p.

Rust, B.R., 1978, Depositional models for braided alluvium, *in* Miall, A.D., ed., Fluvial sedimentology: Canadian Society of Petroleum Geologists Memoir 5, p. 605–625.

Smith, J.G., 1993, Geologic map of upper Eocene to Holocene volcanic and related rocks in the Cascade Range, Washington: U.S. Geological Survey Miscellaneous Investigation Series Map I-2005, scale 1:500,000.

Snavely, P.D., Jr., Brown, R.D., Jr., Roberts, A.E., and Rau, W.W., 1958, Geology and coal resources of the Centralia-Chehalis district, Washington: U.S. Geological Survey Bulletin 1053, 159 p.

Swanson, R.D., McFarland, W.D., Gonthier, J.B., and Wilkinson, J.M., 1993, A description of hydrogeologic units in the Portland Basin, Oregon and Washington: U.S. Geological Survey Water-Resources Investigations Report 90-4196, 56 p., scale 1:100,000.

Tolan T.L., and Beeson, M.H., 1984, Intracanyon flows of the Columbia River Basalt Group in the lower Columbia River Gorge and their relationship to the Troutdale Formation: Geological Society of America Bulletin, v. 95, p. 463–477.

Tolan T.L., and Beeson, M.H., 1999, Geologic map of the Scotts Mills, Silverton, and Slayton Northeast 7.5-minute quadrangles, northwest Oregon: U.S. Geological Survey Open-File Report 99-141, scale 1:24,000 [http://geopubs.wr.usgs.gov/open-file/of99-141].

Trimble, D.E., 1963, Geology of Portland, Oregon and adjacent areas: U.S. Geological Survey Bulletin 1119, 119 p., scale 1:62,500.

Van Atta, R.O., and Kelty, K.B., 1985, Scappoose Formation, Columbia County, Oregon—new evidence of age and relation to Columbia River Basalt Group: American Association of Petroleum Geologists Bulletin, v. 69, p. 688–698.

Vessell, R.K., and Davies, D.K., 1981, Nonmarine sedimentation in an active fore arc basin, *in* Ethridge, F.G., and Flores, R.M., eds., Recent and ancient nonmarine depositional environments—models for exploration: Society of Economic Paleontologists and Mineralogists Special Publication 31, p. 31–45.

Waitt, R.B., Jr., 1985, Case for periodic, colossal jökulhlaups from Pleistocene glacial Lake Missoula: Geological Society of America, v. 96, p. 1271–1286.

Waitt, R.B., Jr., 1994, Scores of gigantic, successively smaller Lake Missoula floods through channeled scabland and Columbia valley, *in* Swanson, D.A., and Haugerud, R.A., eds., Geologic field trips in the Pacific Northwest: Seattle, University of Washington Department of Geological Sciences, p. 1K1–1K88.

Waitt, R.B., Jr., 1996, Numerous colossal Missoula Floods through Columbia Gorge and Portland-Vancouver basin [abs.]: Geological Society of America Abstracts with Program, v. 28, no. 5, p. 120–121.

Walsh, T.J., Korosec, M.A., Phillips, W.M., Logan, R.L., and Schasse, H.W., 1987, Geologic map of Washington—southwest quadrant: Washington Division of Geology and Earth Resources Map GM-34, scale 1:250,000.

Weaver, C.S., Grant, W.C., and Shemeta, J.E., 1987, Local crustal extension at Mount St. Helens, Washington: Journal of Geophysical Research, v. 92, p. 10,170–10,178.

Wegmann, K.W., and Walsh, T.J., 2001, Landslide hazards mapping in Cowlitz County—a progress report: Washington Geology, v. 29, no. 1/2, p. 30–33.

Wells, R.E., Weaver, C.S., and Blakely, R.J., 1998, Fore-arc migration in Cascadia and its neotectonic significance: Geology, v. 26, p. 759–762.

Wilkinson, W.D., Lowry, W.D., and Baldwin, E.M., 1946, Geology of the St. Helens quadrangle, Oregon: Oregon Department of Geology and Mineral Industries Bulletin 31, 39 p., scale 1:62,500.

Williams, H., and McBirney, A.R., 1979, Volcanology: San Francisco, Freeman, Cooper and Co., 397 p.

Wise, W.S., 1970, Cenozoic volcanism in the Cascade Mountains of southern Washington: Washington Division of Mines and Geology Bulletin 60, 45 p.

Wong, I.G., Hemphill-Haley, A., Liberty, L.M., and Madin, I.P., 2001, The Portland Hills Fault—an earthquake generator or just another old fault?: Oregon Geology, v. 63, p. 39–50.

Yelin, T.S., and Patton, H.J., 1991, Seismotectonics of the Portland, Oregon, region: Seismological Society of America Bulletin, v. 81, p. 109–130.

Zuffa, G.G., Normark, W.R., Serra, F., and Brunner, C.A., 2000, Turbidite megabeds in an oceanic rift valley recording jökulhlaups of late Pleistocene glacial lakes of the western United States: Journal of Geology, v. 108, p. 253–274.

Table 1. Chemical analyses of volcanic and intrusive rocks, Yacolt 7.5' quadrangle

[X-ray fluorescence analyses. Rock-type names assigned in accordance with IUGS system (Le Maitre, 2002) applied to recalculated analyses. LOI, loss on ignition. Mg#, atomic ratio $100Mg/(Mg+Fe^{2+})$ with Fe^{2+} set to 0.85x Fe^{total}. Modal analyses, secondary minerals counted as primary mineral replaced. -, not present. X-ray fluorescence analyses by D.M. Johnson at GeoAnalytical Laboratory of Washington State University using methods described in Johnson and others (1999)]

Map No.	1	2	3	4	5	6	7	8	9
Field sample No.	**01YC-P335B**	**01YC-P305B**	**01YC-P305A**	**02YC-P427**	**H98Y-84**	**00YC-P179A**	**H98Y-85**	**02YC-P397**	**01YC-P307**
Latitude (N)	46°49.94'	46°48.55'	46°48.70'	46°50.97'	46°46.18'	46°49.85'	46°45.92'	46°46.44'	46°49.45'
Longitude (W)	122°23.94'	122°23.82'	122°23.64'	122°26.22'	122°27.00'	122°25.50'	122°26.22'	122°24.90'	122°23.34'
Map unit	Tbem	Tbem	Tbem	Tbem	Tbem	Tbem	Tbem	Tbem	Tbem
Rock type	Basalt	Basalt	Basalt	Basalt	Basalt	Basalt	Basalt	Basalt	Basalt
Analyses as reported (wt percent)									
SiO_2	49.30	50.09	50.65	50.63	50.81	50.95	50.81	51.19	50.88
TiO_2	1.81	1.32	0.88	1.10	1.25	1.12	1.27	1.95	1.43
Al_2O_3	16.12	17.33	21.01	21.72	20.14	21.67	19.88	16.30	17.85
FeO*	11.66	10.30	7.77	7.94	9.44	8.03	9.54	12.19	11.06
MnO	0.21	0.21	0.14	0.15	0.17	0.15	0.17	0.23	0.19
MgO	5.47	6.62	4.70	3.44	3.82	3.60	3.70	5.04	4.29
CaO	10.10	10.49	11.92	11.41	10.98	11.36	10.91	9.34	10.21
Na_2O	2.89	2.62	2.37	2.82	2.86	2.78	2.85	3.10	2.93
K_2O	0.45	0.24	0.41	0.37	0.38	0.33	0.41	0.37	0.29
P_2O_5	0.27	0.17	0.11	0.11	0.13	0.11	0.13	0.20	0.14
Total	98.27	99.40	99.96	99.69	99.97	100.09	99.67	99.90	99.27
Analyses recalculated volatile-free and normalized to 100% with all Fe as FeO (wt percent)									
SiO_2	50.17	50.39	50.67	50.79	50.82	50.90	50.98	51.24	51.25
TiO_2	1.84	1.33	0.88	1.10	1.25	1.11	1.28	1.95	1.44
Al_2O_3	16.40	17.44	21.02	21.79	20.15	21.65	19.95	16.32	17.98
FeO*	11.86	10.37	7.78	7.96	9.44	8.02	9.57	12.20	11.14
MnO	0.21	0.21	0.14	0.15	0.17	0.15	0.17	0.23	0.19
MgO	5.57	6.66	4.70	3.45	3.82	3.60	3.71	5.04	4.32
CaO	10.28	10.55	11.93	11.45	10.98	11.35	10.95	9.35	10.28
Na_2O	2.94	2.64	2.37	2.83	2.86	2.78	2.86	3.10	2.95
K_2O	0.46	0.24	0.41	0.37	0.38	0.33	0.41	0.37	0.29
P_2O_5	0.27	0.17	0.11	0.11	0.13	0.11	0.13	0.20	0.14
Mg#	49.6	57.4	55.9	47.6	45.9	48.5	44.9	46.4	44.9
Modes (volume percent)									
Plagioclase	21.3	18.5	30.8	41.9	32.3	55.0	29.0	1.6	19.1
Clinopyroxene	-	-	-	-	-	-	-	-	-
Orthopyroxene	-	-	-	-	-	-	-	-	-
Olivine	2.5	4.6	0.5	0.8	0.1	0.7	0.1	-	0.5
Fe-Ti Oxide	-	-	-	-	-	-	-	trace	-
Hornblende	-	-	-	-	-	-	-	-	-
Biotite	-	-	-	-	-	-	-	-	-
Quartz	-	-	-	-	-	-	-	-	-
K-feldspar	-	-	-	-	-	-	-	-	-
Other	-	-	-	-	-	-	-	-	-
Groundmass	76.2	76.9	68.7	57.3	67.6	44.3	70.9	98.4	80.4
No. points counted	800	812	812.0	800	800	820	788	800.0	812.0
Texture (rock/ groundmass)	seriate/ intergranular	seriate/ intergranular	porphyritic/ intergranular	porphyritic/ intergranular	porphyritic/ cryptocrystalline	seriate/ intergranular	porphyritic/ cryptocrystalline	seriate/ trachytic	porphyritic/ intergranular
Trace element analyses (ppm)									
Ba	137	123	97	90	107	116	125	139	123
Rb	6	2	11	8	7	5	8	2	3
Sr	312	313	321	330	320	334	316	284	297
Y	32	21	23	18	21	21	23	30	26
Zr	155	89	63	58	69	60	69	96	77
Nb	11.1	7.5	4.9	4.6	5.3	3.4	5.2	8.1	6.3
Ni	49	73	16	12	10	9	10	17	11
Cu	232	136	85	139	143	109	149	256	152
Zn	105	82	60	73	78	72	79	113	94
Cr	82	154	72	25	25	28	30	45	53

Table 1. Chemical analyses of volcanic and intrusive rocks, Yacolt 7.5' quadrangle—Continued

Map No.	10	11	12	13	14	15	16	17	18
Field sample No.	**02YC-P408**	**01YC-P369**	**01YC-P250**	**00YC-P182B**	**01YC-P373**	**00YC-P184**	**01YC-P268**	**01YC-P331A**	**01YC-P371**
Latitude (N)	46°50.48'	46°45.60'	46°50.16'	46°49.49'	46°50.17'	46°49.46'	46°47.70'	46°49.36'	46°45.76'
Longitude (W)	122°23.16'	122°24.42'	122°26.40'	122°25.44'	122°27.84'	122°25.08'	122°23.40'	122°23.04'	122°26.28'
Map unit	Tbem	Tbem	Tbem	Tbem	Tbem	Tvb*	Tbem	Tbem	Tbem
Rock type	Basalt	Basalt	Basalt	Basalt	Basalt	Basalt	Basalt	Basalt	Basalt
Analyses as reported (wt percent)									
SiO_2	51.28	51.03	51.13	51.08	51.15	51.88	51.73	51.48	51.62
TiO_2	1.10	1.28	1.52	1.09	1.56	1.06	1.29	1.80	1.54
Al_2O_3	20.51	20.20	17.19	21.73	16.77	22.43	18.87	14.78	18.92
FeO*	7.64	9.12	10.88	7.23	11.35	6.79	8.77	12.75	9.28
MnO	0.15	0.17	0.19	0.15	0.20	0.14	0.15	0.24	0.17
MgO	4.71	3.59	4.90	3.24	4.78	3.27	4.94	4.97	3.92
CaO	11.23	10.39	10.04	11.10	9.82	11.40	10.50	9.56	10.03
Na_2O	2.88	3.02	3.01	2.98	3.04	2.81	2.93	3.06	3.14
K_2O	0.28	0.35	0.43	0.38	0.40	0.36	0.43	0.43	0.53
P_2O_5	0.12	0.13	0.13	0.14	0.14	0.14	0.16	0.16	0.20
Total	99.91	99.28	99.43	99.12	99.20	100.28	99.77	99.23	99.35
Analyses recalculated volatile-free and normalized to 100% with all Fe as FeO (wt percent)									
SiO_2	51.33	51.40	51.43	51.53	51.56	51.74	51.85	51.88	51.96
TiO_2	1.10	1.29	1.52	1.10	1.57	1.05	1.29	1.81	1.55
Al_2O_3	20.53	20.35	17.29	21.92	16.91	22.37	18.91	14.90	19.04
FeO*	7.64	9.12	10.88	7.23	11.35	6.79	8.77	12.75	9.28
MnO	0.15	0.17	0.19	0.15	0.20	0.14	0.15	0.24	0.17
MgO	4.71	3.59	4.90	3.24	4.78	3.27	4.94	4.97	3.92
CaO	11.23	10.39	10.04	11.10	9.82	11.40	10.50	9.56	10.03
Na_2O	2.88	3.02	3.01	2.98	3.04	2.81	2.93	3.06	3.14
K_2O	0.28	0.35	0.43	0.38	0.40	0.36	0.43	0.43	0.53
P_2O_5	0.12	0.13	0.13	0.14	0.14	0.14	0.16	0.16	0.20
Mg#	56.4	45.2	48.6	48.4	46.9	50.2	54.1	45.0	47.0
Modes (volume percent)									
Plagioclase	29.1	39.4	16.4	45.0	10.3	45.8	23.1	0.3	32.3
Clinopyroxene	trace	-	0.3	0.1	-	-	trace	trace	-
Orthopyroxene	-	-	-	-	-	-	-	-	-
Olivine	0.7	0.3	0.5	1.1	0.6	1.1	2.0	-	0.3
Fe-Ti Oxide	-	-	-	-	-	-	-	-	-
Hornblende	-	-	-	-	-	-	-	-	-
Biotite	-	-	-	-	-	-	-	-	-
Quartz	-	-	-	-	-	-	-	-	-
K-feldspar	-	-	-	-	-	-	-	-	-
Other	-	-	-	-	-	-	-	-	-
Groundmass	70.2	60.3	82.8	53.8	89.1	53.1	74.9	99.7	67.4
No. points counted	800	812	812	797	809	810	782	800	800
Texture (rock/ groundmass)	porphyritic/ intergranular	seriate/ microgranular	seriate/ intergranular	seriate/ trachytic	seriate/ trachytic	aphyric/ intersertal	seriate/ intergranular	aphyric/ trachytic	seriate/ intergranular
Trace element analyses (ppm)									
Ba	105	106	126	107	131	105	109	139	145
Rb	2	4	7	7	5	8	9	7	11
Sr	339	328	293	364	284	365	348	256	328
Y	20	21	23	20	23	18	18	29	25
Zr	75	67	70	74	72	70	87	85	109
Nb	5.5	8.6	4.8	5.9	8.1	4.8	7.2	6.7	10.1
Ni	22	11	12	10	16	9	25	10	23
Cu	116	164	146	99	172	225	177	207	128
Zn	70	80	95	69	94	61	81	110	93
Cr	40	26	74	20	70	19	63	69	52

* Sample is from block in tuff breccia.

Table 1. Chemical analyses of volcanic and intrusive rocks, Yacolt 7.5' quadrangle—Continued

Map No.	19	20	21	22	23	24	25	26	27
Field sample No.	**02YC-P453**	**02YC-P440A**	**01YC-P266**	**01YC-P314**	**01YC-P261**	**02YC-P422**	**01YC-P260**	**01YC-P365**	**01YC-P246**
Latitude (N)	46°47.00'	46°49.57'	46°47.75'	46°46.01'	46°47.02'	46°50.65'	46°46.44'	46°45.15'	46°51.22'
Longitude (W)	122°23.64'	122°24.66'	122°26.88'	122°23.46'	122°26.10'	122°25.92'	122°25.08'	122°24.78'	122°24.48'
Map unit	Tbem	Tbem	Tbem	Tbem	Tbem	Tbem	Tbem	Tbem	Tbem
Rock type	Basaltic andesite	Basaltic andesite	Basaltic andesite	Basaltic andesite	Basaltic andesite	Basaltic andesite	Basaltic andesite	Basaltic andesite	Basaltic andesite
Analyses as reported (wt percent)									
SiO_2	51.88	51.88	52.17	51.69	51.59	51.93	51.73	51.94	51.98
TiO_2	1.08	1.55	1.55	1.70	1.89	2.07	1.44	1.69	1.33
Al_2O_3	19.71	16.80	16.29	15.40	15.61	15.45	19.23	15.72	17.19
FeO*	7.96	11.06	11.93	12.49	11.85	12.27	9.20	11.93	9.83
MnO	0.16	0.21	0.22	0.22	0.23	0.23	0.15	0.23	0.18
MgO	4.92	4.83	4.77	4.81	4.66	4.62	3.41	4.80	4.92
CaO	10.78	9.61	9.21	8.92	8.94	8.78	10.11	9.26	10.23
Na_2O	2.77	3.05	3.31	3.15	3.33	3.28	3.13	3.24	2.96
K_2O	0.37	0.43	0.40	0.47	0.51	0.57	0.43	0.40	0.58
P_2O_5	0.13	0.15	0.16	0.16	0.19	0.21	0.14	0.15	0.17
Total	99.76	99.56	100.01	99.02	98.80	99.41	98.98	99.36	99.36
Analyses recalculated volatile-free and normalized to 100% with all Fe as FeO (wt percent)									
SiO_2	52.00	52.11	52.17	52.20	52.22	52.24	52.26	52.28	52.31
TiO_2	1.09	1.55	1.55	1.72	1.91	2.08	1.46	1.70	1.34
Al_2O_3	19.76	16.87	16.29	15.55	15.80	15.54	19.43	15.82	17.30
FeO*	7.98	11.11	11.93	12.61	11.99	12.35	9.30	12.00	9.89
MnO	0.16	0.21	0.22	0.23	0.23	0.23	0.15	0.23	0.18
MgO	4.93	4.85	4.77	4.86	4.72	4.65	3.45	4.83	4.95
CaO	10.81	9.65	9.21	9.01	9.05	8.83	10.21	9.32	10.30
Na_2O	2.78	3.06	3.31	3.18	3.37	3.30	3.16	3.26	2.98
K_2O	0.4	0.4	0.4	0.5	0.5	0.6	0.43	0.40	0.58
P_2O_5	0.13	0.15	0.16	0.16	0.19	0.21	0.14	0.15	0.17
Mg#	56.5	47.8	45.6	44.7	45.2	44.1	43.7	45.8	51.2
Modes (volume percent)									
Plagioclase	33.6	7.0	6.8	0.2	0.8	0.8	33.9	2.0	13.1
Clinopyroxene	1.5	-	-	-	-	-	-	trace	0.9
Orthopyroxene	-	-	-	-	-	-	-	-	0.2
Olivine	1.5	0.7	0.2	-	0.1	0.1	0.1	0.1	0.1
Fe-Ti Oxide	-	trace	-	-	-	-	-	trace	-
Hornblende	-	-	-	-	-	-	-	-	-
Biotite	-	-	-	-	-	-	-	-	-
Quartz	-	-	-	-	-	-	-	-	-
K-feldspar	-	-	-	-	-	-	-	-	-
Other	-	-	-	-	-	-	-	-	-
Groundmass	63.4	92.3	93.0	99.8	99.1	99.1	66.0	97.9	85.7
No. points counted	808	800	810	800	800	800	812	800	816
Texture (rock/ groundmass)	seriate/ intergranular	porphyritic/ trachytic	glomerophyric/ intergranular	aphryic/ trachytic	sparsely phyric/ trachytic	sparsely phyric/ intergranular	glomerophyric/ intergranular	sparsely phyric/ trachytic	seriate/ intergranular
Trace element analyses (ppm)									
Ba	98	123	156	147	158	159	115	128	151
Rb	8	6	3	9	6	13	9	6	13
Sr	335	273	290	259	280	269	318	262	306
Y	17	25	26	28	30	33	22	27	27
Zr	74	80	91	88	103	104	75	74	114
Nb	5.7	5.6	7.2	6.9	8.4	7.7	5.3	9.1	7.2
Ni	21	13	12	9	10	10	10	11	14
Cu	120	198	171	232	212	223	210	209	149
Zn	73	99	103	110	114	116	96	102	86
Cr	49	50	37	58	46	47	35	60	34

Table 1. Chemical analyses of volcanic and intrusive rocks, Yacolt 7.5' quadrangle—Continued

Map No.	28	29	30	31	32	33	34	35	36
Field sample No.	**01YC-P302A**	**01YC-P262**	**01YC-P248**	**01YC-P317**	**01YC-P267**	**01YC-P379**	**02YC-P444**	**01YC-P304**	**00YC-P176**
Latitude (N) Longitude (W)	46°48.04' 122°22.86'	46°47.46' 122°25.08'	46°52.27' 122°30.00'	46°45.51' 122°24.18'	46°47.08' 122°23.22'	46°45.50' 122°25.74'	46°47.63' 122°26.64'	46°48.47' 122°25.58'	46°48.29' 122°23.94'
Map unit	Tbem	Tbem	Tbem	Tbem	Tbem	Tbem	Tbem	Tbem	Tbem
Rock type	Basaltic andesite	Basaltic andesite	Basaltic andesite	Basaltic andesite	Basaltic andesite	Basaltic andesite	Basaltic andesite	Basaltic andesite	Basaltic andesite
Analyses as reported (wt percent)									
SiO_2	52.28	52.23	51.96	52.15	52.60	52.61	52.46	52.67	52.45
TiO_2	1.58	1.56	1.25	1.95	1.61	1.67	1.67	1.26	1.30
Al_2O_3	16.03	16.20	19.89	17.33	15.83	15.60	15.78	17.65	17.38
FeO*	12.04	11.85	8.61	10.49	12.20	12.22	11.22	8.95	9.05
MnO	0.22	0.20	0.17	0.21	0.22	0.25	0.24	0.16	0.17
MgO	4.61	4.72	3.48	3.78	4.72	4.57	4.77	4.96	5.00
CaO	9.30	8.88	9.93	9.36	8.71	9.04	9.48	10.32	9.95
Na_2O	3.24	3.31	3.16	3.32	3.35	3.27	3.17	2.87	2.91
K_2O	0.48	0.50	0.47	0.43	0.53	0.33	0.41	0.52	0.72
P_2O_5	0.15	0.16	0.16	0.19	0.17	0.16	0.16	0.21	0.22
Total	99.92	99.60	99.08	99.21	99.94	99.71	99.36	99.58	99.14
Analyses recalculated volatile-free and normalized to 100% with all Fe as FeO (wt percent)									
SiO_2	52.32	52.44	52.44	52.56	52.63	52.77	52.80	52.89	52.91
TiO_2	1.58	1.56	1.26	1.97	1.61	1.67	1.68	1.27	1.31
Al_2O_3	16.04	16.27	20.07	17.47	15.84	15.65	15.88	17.73	17.53
FeO*	12.04	11.89	8.69	10.58	12.21	12.25	11.29	8.99	9.13
MnO	0.22	0.20	0.17	0.21	0.22	0.25	0.24	0.16	0.17
MgO	4.61	4.74	3.51	3.81	4.72	4.58	4.80	4.98	5.04
CaO	9.31	8.92	10.02	9.43	8.72	9.07	9.54	10.36	10.04
Na_2O	3.24	3.32	3.19	3.35	3.35	3.28	3.19	2.88	2.94
K_2O	0.48	0.50	0.47	0.43	0.53	0.33	0.41	0.52	0.73
P_2O_5	0.15	0.16	0.16	0.19	0.17	0.16	0.16	0.21	0.22
Mg#	44.6	45.5	45.9	43.0	44.8	44.0	47.1	53.8	53.7
Modes (volume percent)									
Plagioclase	4.5	5.3	33.7	15.6	5.4	0.3	0.8	19.9	18.4
Clinopyroxene	0.1	-	1.7	-	-	-	-	0.1	0.1
Orthopyroxene	-	-	-	-	-	-	-	-	-
Olivine	-	0.5	2.9	0.6	0.3	-	0.1	0.8	0.9
Fe-Ti Oxide	-	trace	0.2	-	trace	-	-	-	-
Hornblende	-	-	-	-	-	-	-	-	-
Biotite	-	-	-	-	-	-	-	-	-
Quartz	-	-	-	-	-	-	-	-	-
K-feldspar	-	-	-	-	-	-	-	-	-
Other	-	-	-	-	-	-	-	-	-
Groundmass	95.1	94.2	61.5	83.8	94.3	99.7	99.1	79.2	80.6
No. points counted	800	810	804	800	800	800	800	810	798
Texture (rock/ groundmass)	seriate/ intergranular	sparsely phyric/ intergranular	seriate/ intergranular	porphyritic/ trachytic	sparsely phyric/ intergranular	aphryic/ trachytic	sparsely phyric/ trachytic	porphyritic/ intergranular	porphyritic/ trachytic
Trace element analyses (ppm)									
Ba	134	135	125	149	149	139	166	155	172
Rb	10	11	10	4	11	7	4	20	18
Sr	279	277	314	295	275	274	275	295	285
Y	25	25	22	44	29	30	28	27	28
Zr	76	90	95	101	93	84	87	124	127
Nb	6.0	6.9	7.0	8.4	7.1	8.1	6.9	8.5	8.6
Ni	11	9	8	13	9	12	12	33	33
Cu	98	208	127	214	438	234	211	112	105
Zn	101	103	87	134	110	111	108	77	80
Cr	53	36	28	48	40	36	52	94	95

Table 1. Chemical analyses of volcanic and intrusive rocks, Yacolt 7.5' quadrangle—Continued

Map No.	37	38	39	40	41	42	43	44	45
Field sample No.	**02YC-P416**	**01YC-P271**	**01YC-P363B**	**H98Y-82**	**02YC-P445**	**02YC-P396A**	**01YC-P270**	**02YC-P472A**	**02YC-P430**
Latitude (N) Longitude (W)	46°50.39' 122°28.26'	46°45.55' 122°22.50'	46°50.36' 122°25.56'	46°48.03' 122°26.76'	46°47.72' 122°25.98'	46°46.39' 122°26.70'	46°45.95' 122°22.62'	46°47.62' 122°27.12'	46°48.95' 122°22.98'
Map unit	Tbem	Tbem	Tba	Tbem	Tbem	Tbem	Tbem	Tbem	Tbem
Rock type	Basaltic andesite	Basaltic andesite	Basaltic andesite	Basaltic andesite	Basaltic andesite	Basaltic andesite	Basaltic andesite	Basaltic andesite	Basaltic andesite
Analyses as reported (wt percent)									
SiO_2	52.88	52.62	52.46	52.47	52.82	53.02	52.85	53.19	53.67
TiO_2	1.53	1.35	1.26	1.58	1.62	1.73	1.57	1.65	1.32
Al_2O_3	16.65	17.19	17.91	15.91	16.23	15.19	15.69	16.58	18.71
FeO*	11.20	10.40	9.10	11.75	11.33	12.50	11.49	10.46	9.22
MnO	0.21	0.19	0.16	0.22	0.22	0.23	0.22	0.22	0.18
MgO	4.46	4.61	4.86	4.60	4.41	4.58	4.54	4.22	3.67
CaO	9.04	9.41	9.53	8.56	8.72	8.41	8.84	8.88	9.24
Na_2O	3.26	3.02	2.98	3.31	3.30	3.29	3.39	3.45	3.31
K_2O	0.55	0.47	0.62	0.47	0.50	0.57	0.34	0.52	0.51
P_2O_5	0.18	0.13	0.19	0.17	0.18	0.19	0.17	0.18	0.15
Total	99.94	99.38	99.08	99.04	99.33	99.70	99.10	99.35	99.97
Analyses recalculated volatile-free and normalized to 100% with all Fe as FeO (wt percent)									
SiO_2	52.91	52.95	52.95	52.98	53.18	53.18	53.33	53.54	53.69
TiO_2	1.53	1.36	1.28	1.60	1.63	1.73	1.59	1.66	1.32
Al_2O_3	16.66	17.30	18.08	16.06	16.34	15.24	15.83	16.69	18.72
FeO*	11.20	10.46	9.19	11.86	11.41	12.53	11.60	10.52	9.22
MnO	0.21	0.19	0.16	0.23	0.23	0.23	0.22	0.23	0.18
MgO	4.46	4.64	4.91	4.64	4.44	4.59	4.58	4.25	3.67
CaO	9.05	9.47	9.62	8.64	8.78	8.44	8.92	8.94	9.24
Na_2O	3.26	3.04	3.01	3.34	3.32	3.30	3.42	3.47	3.31
K_2O	0.55	0.47	0.63	0.47	0.50	0.57	0.34	0.52	0.51
P_2O_5	0.18	0.13	0.19	0.17	0.18	0.19	0.17	0.18	0.15
Mg#	45.5	48.2	52.8	45.1	44.9	43.5	45.3	45.8	45.5
Modes (volume percent)									
Plagioclase	4.5	15.5	18.4	3.0	2.5	0.3	trace	2.6	22.2
Clinopyroxene	-	-	0.6	-	-	-	trace	-	0.3
Orthopyroxene	-	-	-	-	-	-	-	-	-
Olivine	-	0.5	3.8	-	0.4	-	trace	0.4	0.5
Fe-Ti Oxide	-	-	trace	0.1	-	-	-	-	-
Hornblende	-	-	-	-	-	-	-	-	-
Biotite	-	-	-	-	-	-	-	-	-
Quartz	-	-	-	-	-	-	-	-	-
K-feldspar	-	-	-	-	-	-	-	-	-
Other	-	-	-	-	-	-	-	-	-
Groundmass	95.5	84.0	77.2	96.9	97.1	99.7	100.0	97.0	77.0
No. points counted	800	800	820	800	800	800	800	800	820
Texture (rock/ groundmass)	sparsely phyric/ trachytic	seriate/ intergranular	seriate/ intergranular	seriate/ intergranular	sparsely phyric/ trachytic	aphryic/ trachytic	aphyric/ trachytic	sparsely phyric/ trachytic	porphyritic/ intergranular
Trace element analyses (ppm)									
Ba	149	125	161	136	139	162	145	162	127
Rb	8	11	14	7	7	11	3	10	13
Sr	277	296	305	270	273	261	291	283	310
Y	26	21	27	27	27	29	29	29	22
Zr	96	83	131	94	93	103	96	97	92
Nb	7.5	6.2	8.7	7.9	7.0	8.2	6.8	8.6	7.0
Ni	10	7	42	14	9	14	5	10	5
Cu	157	203	130	167	166	272	174	239	104
Zn	103	90	83	106	105	115	99	117	84
Cr	34	28	40	35	34	27	52	32	21

Table 1. Chemical analyses of volcanic and intrusive rocks, Yacolt 7.5' quadrangle—Continued

Map No.	46	47	48	49	50	51	52	53	54
Field sample No.	**01YC-P264**	**01YC-P257**	**01YC-P343**	**01YC-P341**	**01YC-P330**	**00YC-P181**	**01YC-P258**	**02YC-P449**	**02YC-P411s**
Latitude (N) Longitude (W)	46°47.69' 122°24.78'	46°50.00' 122°23.82'	46°50.08' 122°25.08'	46°49.42' 122°22.62'	46°49.52' 122°22.98'	46°49.65' 122°25.26'	46°50.06' 122°24.24'	46°48.05' 122°25.74'	46°48.08' 122°24.72'
Map unit	Tbem	Tbem	Tbem	Tbem	Tbem	Tbem	Qls*	Tbem	Tbem
Rock type	Basaltic andesite	Basaltic andesite	Basaltic andesite	Basaltic andesite	Basaltic andesite	Basaltic andesite	Basaltic andesite	Basaltic andesite	Basaltic andesite
Analyses as reported (wt percent)									
SiO_2	53.33	53.39	53.24	53.70	53.91	54.20	53.65	54.08	54.33
TiO_2	1.65	1.59	1.45	1.40	1.52	1.34	1.85	1.62	1.52
Al_2O_3	15.02	17.36	16.97	17.56	16.97	18.67	15.41	15.40	16.93
FeO*	12.45	9.78	9.43	9.18	9.69	8.66	11.29	11.52	9.07
MnO	0.25	0.19	0.19	0.18	0.19	0.19	0.20	0.22	0.18
MgO	3.96	3.54	4.17	4.01	4.05	3.44	3.80	4.04	4.37
CaO	8.32	8.69	8.82	9.16	8.49	9.40	7.92	8.36	9.35
Na_2O	3.50	3.67	3.51	3.21	3.61	3.32	3.81	3.45	3.02
K_2O	0.57	0.59	0.57	0.61	0.59	0.51	0.65	0.55	0.73
P_2O_5	0.15	0.21	0.32	0.22	0.34	0.15	0.23	0.15	0.26
Total	99.19	99.02	98.67	99.23	99.36	99.88	98.82	99.39	99.76
Analyses recalculated volatile-free and normalized to 100% with all Fe as FeO (wt percent)									
SiO_2	53.76	53.92	53.96	54.12	54.26	54.27	54.29	54.41	54.46
TiO_2	1.66	1.61	1.47	1.41	1.53	1.34	1.88	1.62	1.52
Al_2O_3	15.14	17.53	17.20	17.70	17.08	18.69	15.59	15.50	16.97
FeO*	12.55	9.88	9.55	9.25	9.76	8.67	11.43	11.59	9.09
MnO	0.25	0.19	0.19	0.18	0.19	0.19	0.20	0.22	0.18
MgO	3.99	3.58	4.23	4.04	4.08	3.44	3.85	4.06	4.38
CaO	8.39	8.78	8.94	9.23	8.54	9.41	8.01	8.41	9.37
Na_2O	3.53	3.71	3.56	3.24	3.63	3.32	3.86	3.47	3.03
K_2O	0.57	0.60	0.58	0.61	0.59	0.51	0.66	0.55	0.73
P_2O_5	0.15	0.21	0.3	0.2	0.34	0.15	0.24	0.15	0.26
Mg#	40.0	43.2	48.1	47.8	46.7	45.4	41.4	42.4	50.3
Modes (volume percent)									
Plagioclase	0.2	20.1	11.4	15.7	9.1	-	2.4	-	19.0
Clinopyroxene	trace	0.4	-	1.1	trace	-	-	-	1.9
Orthopyroxene	-	-	-	-	-	-	-	-	0.5
Olivine	trace	0.1	0.4	2.7	0.2	-	-	-	0.3
Fe-Ti Oxide	-	trace	-	-	-	-	-	-	-
Hornblende	-	-	-	-	-	-	-	-	-
Biotite	-	-	-	-	-	-	-	-	-
Quartz	-	-	-	-	-	-	-	-	-
K-feldspar	-	-	-	-	-	-	-	-	-
Other	-	-	-	-	-	-	-	-	-
Groundmass	99.8	79.4	88.2	80.5	90.7	100.0	97.6	100.0	78.3
No. points counted	800	800	800	785	812	-	800	-	810
Texture (rock/ groundmass)	microphyric/ intergranular	seriate/ intergranular	seriate/ trachytic	seriate/ intergranular	seriate/ trachytic	aphyric/ trachytic	sparsely phyric/ trachytic	aphryic/ intergranular	glomerophyric/ intersertal
Trace element analyses (ppm)									
Ba	149	163	161	188	160	188	175	139	204
Rb	14	14	13	8	11	14	13	11	23
Sr	267	318	297	306	300	267	294	261	275
Y	28	29	29	29	31	31	36	26	34
Zr	95	121	98	149	105	109	132	92	165
Nb	6.4	8.4	7.8	9.9	7.7	6.0	9.1	6.9	12.0
Ni	4	3	10	13	9	2	6	4	21
Cu	259	137	151	128	130	219	179	187	152
Zn	111	91	91	87	93	104	109	99	90
Cr	26	22	56	27	48	16	25	19	45

* Sample is from block in landslide.

Table 1. Chemical analyses of volcanic and intrusive rocks, Yacolt 7.5' quadrangle—Continued

Map No.	55	56	57	58	59	60	61	62	63
Field sample No.	**02YC-P419**	**02YC-P460**	**01YC-P336A**	**01YC-P342**	**02YC-P459A**	**01YC-P358B**	**02YC-P420**	**01YC-P319**	**00YC-P183**
Latitude (N) Longitude (W)	46°50.26' 122°24.72'	46°48.70' 122°24.54'	46°49.83' 122°24.12'	46°49.85' 122°23.04'	46°48.85' 122°24.06'	46°50.39' 122°26.58'	46°50.50' 122°25.56'	46°46.25' 122°22.74'	46°49.42' 122°24.42'
Map unit	Tbem	Tbem	Tbem	Tbem	Tbem	Tbem	Tbem	Tbem	Tvb*
Rock type	Basaltic andesite	Basaltic andesite	Basaltic andesite	Basaltic andesite	Basaltic andesite	Basaltic andesite	Basaltic andesite	Basaltic andesite	Basaltic andesite
Analyses as reported (wt percent)									
SiO_2	54.07	54.37	54.21	54.14	54.45	54.24	54.47	54.25	54.74
TiO_2	1.61	1.49	1.83	1.82	1.45	1.84	1.51	1.43	1.72
Al_2O_3	17.50	16.47	15.48	15.38	16.18	16.12	17.21	17.02	15.26
FeO*	9.19	9.74	11.20	11.20	9.80	9.92	8.76	9.61	11.75
MnO	0.18	0.18	0.19	0.21	0.17	0.20	0.18	0.17	0.22
MgO	3.51	4.20	3.85	3.78	4.33	4.17	4.05	3.46	3.84
CaO	8.72	9.10	7.86	7.82	8.92	8.06	8.91	9.20	7.81
Na_2O	3.57	3.04	3.82	3.78	3.02	3.67	3.32	3.00	3.55
K_2O	0.58	0.78	0.64	0.64	0.93	0.62	0.79	0.60	0.64
P_2O_5	0.21	0.26	0.23	0.23	0.25	0.22	0.24	0.20	0.18
Total	99.15	99.62	99.31	98.99	99.49	99.06	99.43	98.94	99.70
Analyses recalculated volatile-free and normalized to 100% with all Fe as FeO (wt percent)									
SiO_2	54.53	54.58	54.59	54.69	54.73	54.76	54.78	54.83	54.90
TiO_2	1.63	1.49	1.84	1.84	1.45	1.86	1.51	1.44	1.72
Al_2O_3	17.65	16.53	15.59	15.54	16.26	16.27	17.31	17.20	15.31
FeO*	9.27	9.77	11.27	11.31	9.85	10.01	8.81	9.71	11.79
MnO	0.18	0.18	0.19	0.21	0.17	0.20	0.19	0.17	0.22
MgO	3.54	4.22	3.88	3.82	4.35	4.21	4.07	3.50	3.85
CaO	8.79	9.14	7.91	7.90	8.97	8.14	8.96	9.30	7.83
Na_2O	3.60	3.05	3.85	3.82	3.04	3.70	3.34	3.03	3.56
K_2O	0.58	0.78	0.64	0.65	0.93	0.63	0.79	0.61	0.64
P_2O_5	0.21	0.26	0.23	0.23	0.25	0.22	0.24	0.20	0.18
Mg#	44.5	47.5	41.9	41.5	48.1	46.9	49.2	43.0	40.7
Modes (volume percent)									
Plagioclase	14.0	20.5	1.8	1.8	6.3	3.8	14.3	20.5	20.5
Clinopyroxene	trace	2.4	-	-	0.6	-	0.6	1.1	trace
Orthopyroxene	-	0.4	-	-	-	-	-	0.5	-
Olivine	0.3	0.6	-	-	0.2	0.2	1.2	0.4	0.4
Fe-Ti Oxide	trace	-	-	trace	-	-	-	-	-
Hornblende	-	-	-	-	-	-	-	-	-
Biotite	-	-	-	-	-	-	-	-	-
Quartz	-	-	-	-	-	-	-	-	-
K-feldspar	-	-	-	-	-	-	-	-	-
Other	-	-	-	-	-	-	-	-	-
Groundmass	85.7	76.1	98.2	98.2	92.9	96.0	83.9	77.5	79.1
No. points counted	800	800	810	800	786	800	800	812	800
Texture (rock/ groundmass)	seriate/ intergranular	seriate/ intergranular	sparsely phyric/ trachytic	sparsely phyric/ trachytic	seriate/ trachytic	sparsely phyric/ trachytic	seriate/ intergranular	seriate/ trachytic	porphyritic/ trachytic
Trace element analyses (ppm)									
Ba	155	205	174	165	205	167	184	197	147
Rb	11	19	13	14	27	13	21	21	12
Sr	309	277	291	288	271	289	290	299	313
Y	29	35	32	32	34	30	32	33	24
Zr	118	170	129	129	158	110	148	154	93
Nb	9.4	12.1	9.8	9.2	9.4	8.1	10.7	9.5	4.8
Ni	7	19	7	4	18	10	14	10	5
Cu	243	148	288	175	67	157	98	158	111
Zn	94	90	104	105	87	99	89	84	79
Cr	17	46	20	22	49	38	34	21	26

* Sample is from block in tuff breccia.

Table 1. Chemical analyses of volcanic and intrusive rocks, Yacolt 7.5' quadrangle—Continued

Map No.	64	65	66	67	68	69	70	71	72
Field sample No.	**00YC-P185**	**02YC-P414**	**02YC-P429**	**00YC-P187**	**01YC-P251**	**00YC-P178B**	**01YC-P338**	**00YC-P174**	**02YC-P436A**
Latitude (N) Longitude (W)	46°49.14' 122°25.26'	46°49.12' 122°23.52'	46°48.73' 122°22.86'	46°49.34' 122°24.84'	46°49.91' 122°28.14'	46°47.43' 122°23.22'	46°49.95' 122°24.66'	46°52.36' 122°23.46'	46°49.25' 122°27.24'
Map unit	Tbem	Tbem	Tbem	Tbem	Tbem	Tbem	Tbem	Tbem	Tbem
Rock type	Basaltic andesite	Basaltic andesite	Basaltic andesite	Basaltic andesite	Basaltic andesite	Basaltic andesite	Basaltic andesite	Basaltic andesite	Basaltic andesite
Analyses as reported (wt percent)									
SiO_2	54.65	55.12	54.87	55.16	54.70	54.69	55.05	55.39	55.42
TiO_2	1.49	1.48	1.73	1.32	1.66	1.59	1.56	1.81	1.68
Al_2O_3	16.42	16.36	15.44	17.66	15.15	15.13	16.63	15.76	15.60
FeO*	9.36	9.33	11.05	8.97	11.44	11.50	9.51	10.43	10.93
MnO	0.18	0.20	0.22	0.17	0.23	0.23	0.18	0.19	0.23
MgO	4.16	4.56	4.06	3.85	3.53	3.81	3.68	3.80	3.63
CaO	9.22	8.72	7.70	8.40	7.47	7.39	8.14	8.03	7.60
Na_2O	2.99	3.04	3.60	3.50	3.83	3.63	3.71	3.59	3.67
K_2O	0.77	0.94	0.64	0.66	0.70	0.69	0.62	0.62	0.67
P_2O_5	0.26	0.26	0.18	0.22	0.19	0.21	0.34	0.24	0.18
Total	99.50	100.01	99.49	99.91	98.89	98.87	99.42	99.84	99.61
Analyses recalculated volatile-free and normalized to 100% with all Fe as FeO (wt percent)									
SiO_2	54.93	55.11	55.15	55.21	55.31	55.32	55.37	55.48	55.64
TiO_2	1.50	1.48	1.73	1.32	1.68	1.61	1.57	1.81	1.69
Al_2O_3	16.50	16.36	15.52	17.68	15.32	15.30	16.73	15.78	15.66
FeO*	9.41	9.33	11.11	8.97	11.57	11.63	9.56	10.44	10.98
MnO	0.18	0.20	0.23	0.17	0.23	0.23	0.18	0.19	0.23
MgO	4.18	4.56	4.08	3.85	3.57	3.85	3.70	3.81	3.64
CaO	9.27	8.72	7.74	8.41	7.55	7.47	8.19	8.04	7.63
Na_2O	3.01	3.04	3.62	3.50	3.87	3.67	3.73	3.60	3.68
K_2O	0.77	0.94	0.64	0.66	0.71	0.70	0.62	0.62	0.67
P_2O_5	0.26	0.26	0.18	0.22	0.19	0.21	0.35	0.24	0.18
Mg#	48.2	50.6	43.5	47.4	39.3	41.0	44.8	43.3	41.1
Modes (volume percent)									
Plagioclase	19.1	5.1	-	19.4	0.2	1.3	9.8	1.2	0.8
Clinopyroxene	2.7	0.4	-	trace	0.1	-	-	0.3	0.3
Orthopyroxene	0.4	-	-	-	-	-	-	-	-
Olivine	0.5	0.5	-	2.6	-	trace	0.2	0.4	trace
Fe-Ti Oxide	-	-	-	-	trace	trace	-	-	trace
Hornblende	-	-	-	-	-	-	-	-	-
Biotite	-	-	-	-	-	-	-	-	-
Quartz	-	-	-	-	-	-	-	-	-
K-feldspar	-	-	-	-	-	-	-	-	-
Other	-	-	-	-	-	-	-	-	-
Groundmass	77.3	94.0	100.0	78.0	99.7	98.7	90.0	98.1	98.9
No. points counted	766	800	-	804	800	800	810	780	800
Texture (rock/ groundmass)	porphyritic/ intersertal	seriate/ intergranular	aphryic/ intergranular	seriate/ trachytic	~aphryic/ trachytic	seriate/ trachytic	porphyritic/ intergranular	seriate/ trachytic	sparsely phyric/ trachytic
Trace element analyses (ppm)									
Ba	208	212	170	181	178	188	168	199	180
Rb	24	25	15	14	15	16	16	14	14
Sr	274	261	261	298	274	256	296	287	274
Y	35	34	30	31	32	37	32	33	35
Zr	170	166	108	130	119	122	111	133	113
Nb	10.3	11.7	8.0	8.4	8.6	8.8	8.3	9.2	8.3
Ni	13	18	4	9	1	6	10	5	3
Cu	136	77	230	51	93	187	51	197	65
Zn	86	89	111	85	109	114	93	98	119
Cr	44	42	12	31	16	28	40	27	10

Table 1. Chemical analyses of volcanic and intrusive rocks, Yacolt 7.5' quadrangle—Continued

Map No.	73	74	75	76	77	78	79	80	81
Field sample No.	**02YC-P454**	**01YC-P269**	**00YC-P166**	**02YC-P438D**	**01YC-P384B**	**02YC-P417**	**02YC-P442B**	**02YC-P436B**	**01YC-P245**
Latitude (N) Longitude (W)	46°47.23' 122°23.70'	46°46.71' 122°22.62'	46°51.71' 122°23.16'	46°49.48' 122°24.36'	46°49.75' 122°26.22'	46°50.38' 122°28.38'	46°49.53' 122°27.06'	46°49.38' 122°27.24'	46°51.61' 122°26.88'
Map unit	Tbem	Tbem	Tbem	Tbem	Tbem	Tbem	Td	Td	Tqdy
Rock type	Basaltic andesite	Basaltic andesite	Basaltic andesite	Basaltic andesite	Basaltic andesite	Andesite	Dacite	Dacite	Pyroxene quartz diorite
Analyses as reported (wt percent)									
SiO_2	55.52	55.50	55.78	56.11	56.00	56.57	62.63	62.73	58.32
TiO_2	1.55	1.57	1.79	1.66	1.59	1.63	1.16	1.13	0.97
Al_2O_3	16.05	16.23	15.81	15.00	15.50	15.76	16.61	16.59	16.90
FeO*	10.36	10.10	10.19	11.22	10.42	9.96	5.92	5.94	6.58
MnO	0.21	0.23	0.19	0.22	0.24	0.21	0.16	0.15	0.11
MgO	3.51	3.46	3.38	3.22	2.91	3.23	1.65	1.80	4.17
CaO	7.71	7.58	7.84	6.77	6.77	6.64	5.04	4.95	7.14
Na_2O	3.81	3.77	3.73	3.84	4.08	4.01	4.91	4.84	3.80
K_2O	0.55	0.65	0.69	0.79	0.66	0.73	1.02	1.02	1.14
P_2O_5	0.17	0.21	0.25	0.22	0.21	0.21	0.28	0.28	0.18
Total	99.44	99.30	99.64	99.04	98.38	98.95	99.38	99.44	99.31
Analyses recalculated volatile-free and normalized to 100% with all Fe as FeO (wt percent)									
SiO_2	55.83	55.89	55.98	56.65	56.92	57.17	63.02	63.08	58.73
TiO_2	1.56	1.58	1.79	1.67	1.62	1.64	1.17	1.14	0.98
Al_2O_3	16.14	16.34	15.87	15.14	15.76	15.93	16.71	16.68	17.02
FeO*	10.42	10.17	10.23	11.32	10.59	10.06	5.96	5.98	6.63
MnO	0.21	0.23	0.19	0.23	0.24	0.22	0.16	0.15	0.11
MgO	3.53	3.48	3.39	3.25	2.96	3.26	1.66	1.81	4.20
CaO	7.75	7.63	7.87	6.84	6.88	6.71	5.07	4.98	7.19
Na_2O	3.83	3.80	3.74	3.88	4.15	4.05	4.94	4.87	3.83
K_2O	0.55	0.65	0.69	0.80	0.67	0.74	1.03	1.03	1.15
P_2O_5	0.17	0.21	0.25	0.22	0.22	0.22	0.28	0.28	0.18
Mg#	41.5	41.8	41.0	37.6	36.9	40.5	36.9	38.8	57.1
Modes (volume percent)									
Plagioclase	0.1	2.9	0.8	-	4.4	4.3	12.8	12.4	64.8
Clinopyroxene	trace	0.3	trace	-	-	trace	1.5	1.0	6.0
Orthopyroxene	-	-	-	-	-	-	1.3	1.0	11.2
Olivine	-	0.3	0.2	-	0.8	0.5	-	-	trace
Fe-Ti Oxide	-	0.1	-	-	0.1	0.1	0.9	0.6	2.1
Hornblende	-	-	-	-	-	-	-	-	0.4
Biotite	-	-	-	-	-	-	-	-	0.6
Quartz	-	-	-	-	-	-	-	-	1.2
K-feldspar	-	-	-	-	-	-	-	-	qtz-fsp: 11.7
Other	-	-	-	-	-	-	-	-	smectite: 2.0
Groundmass	99.9	96.4	99.0	100.0	94.7	95.1	83.5	85.0	0.0
No. points counted	800	800	750	-	812	800	820	800	813
Texture (rock/ groundmass)	aphryic/ trachytic	sparsely phyric/ intergranular	seriate/ trachytic	aphryic/ intergranular	seriate/ intersertal	seriate/ intergranular	glomerophyric/ pilotaxitic	glomerophyric/ pilotaxitic	hypidiomorphic// granular
Trace element analyses (ppm)									
Ba	155	177	191	207	188	186	248	258	312
Rb	10	14	17	18	13	16	19	21	29
Sr	285	290	290	251	283	279	282	272	402
Y	31	35	36	38	32	31	52	39	18
Zr	101	124	136	140	127	126	185	185	161
Nb	8.6	7.8	9.5	9.9	10.9	9.3	13.0	12.1	9.3
Ni	3	3	5	5	1	2	5	5	48
Cu	139	180	176	204	73	74	35	34	25
Zn	105	100	101	117	111	110	97	104	72
Cr	9	16	24	13	9	12	2	7	93

qtz-fsp, fine-grained quartz-feldspar intergrowths.

Table 1. Chemical analyses of volcanic and intrusive rocks, Yacolt 7.5' quadrangle—Continued

Map No.	82	83	84	85
Field sample No.	**02YC-P424**	**H98Y-33**	**01YC-P239**	**01YC-P255**
Latitude (N) Longitude (W)	46°50.89' 122°26.40'	46°48.26' 122°29.70'	46°47.70' 122°29.99'	46°50.48' 122°25.20'
Map unit	Tqdy	Qbbg	Qbbg	Qalf
Rock type	Micro-quartz diorite	Basalt	Basalt	Andesite
		Analyses as reported (wt percent)		
SiO_2	58.85	49.17	48.73	57.65
TiO_2	1.01	1.98	1.84	1.14
Al_2O_3	17.05	16.77	16.40	17.57
FeO*	6.06	8.81	9.71	6.57
MnO	0.11	0.14	0.15	0.10
MgO	3.96	7.32	8.23	3.87
CaO	7.14	9.55	8.86	6.88
Na_2O	3.71	3.45	3.46	4.30
K_2O	1.14	1.27	1.15	0.94
P_2O_5	0.19	0.24	0.44	0.24
Total	99.21	98.70	98.98	99.27
		Analyses recalculated volatile-free and normalized to 100% with all Fe as FeO (wt percent)		
SiO_2	59.32	49.82	49.23	58.07
TiO_2	1.01	2.00	1.86	1.15
Al_2O_3	17.19	16.99	16.57	17.70
FeO*	6.11	8.93	9.81	6.62
MnO	0.11	0.14	0.15	0.10
MgO	3.99	7.42	8.32	3.90
CaO	7.20	9.68	8.95	6.93
Na_2O	3.74	3.50	3.50	4.33
K_2O	1.15	1.29	1.16	0.95
P_2O_5	0.19	0.25	0.45	0.25
Mg#	57.8	63.5	64.0	55.3
		Modes (volume percent)		
Plagioclase	42.0	-	-	-
Clinopyroxene	4.6	-	-	-
Orthopyroxene	3.5	-	-	-
Olivine	1.1	11.3	11.5	-
Fe-Ti Oxide	0.9	-	-	-
Hornblende	-	-	-	-
Biotite	-	-	-	-
Quartz	-	-	-	-
K-feldspar	-	-	-	-
Other	-	-	-	-
Groundmass	47.9	88.7	88.5	100.0
No. points counted	820	800	768	-
Texture (rock/ groundmass)	porphyritic/ intersertal	porphyritic/ intergranular	porphyritic/ intergranular	aphryic/ pilotaxitic
		Trace element analyses (ppm)		
Ba	275	293	270	282
Rb	26	16	11	14
Sr	401	695	710	556
Y	19	16	21	14
Zr	158	177	174	124
Nb	9.6	26.4	22.5	9.3
Ni	45	128	144	54
Cu	81	45	55	56
Zn	72	75	77	90
Cr	92	203	230	77

Table 2. Summary of $^{40}Ar/^{39}Ar$ incremental-heating age determinations, Yacolt 7.5' quadrangle

Field sample no.	Location Latitude (N)	Longitude (W)	Map unit	Rock type	Material dated	Age) (±1σ error)	Source
H98Y-33	45°48.258'	122°29.700'	Qbbg	Basaltic andesite	Whole-rock	99±57 ka	R.J. Fleck, written commun., 2002
02YC-P424	45°50.886'	122°26.400'	Tqdy	Microquartz diorite	Plagioclase	21.5±0.1 Ma	R.J. Fleck, written commun., 2005
01YC-P305A	45°48.696'	122°23.640'	Tbem	Basaltic andesite	Whole-rock	27.1±0.1 Ma	R.J. Fleck, written commun., 2005
02YC-P436B	45°49.380'	122°27.240'	Td	Dacite	Plagioclase	26.4±0.1 Ma	R.J. Fleck, written commun., 2005
01YC-P363B	45°50.364'	122°25.560'	Tba	Basaltic andesite	Plagioclase	31.9±1.2 Ma	R.J. Fleck, written commun., 2005